Integration of Orthogonal Signaling by the Notch and Dpp Pathways in *Drosophila*

Elizabeth Stroebele and Albert Erives[1]
Department of Biology, University of Iowa, Iowa City, Iowa 52242-1324
ORCID ID: 0000-0001-7107-5518 (A.E.)

ABSTRACT The transcription factor Suppressor of Hairless and its coactivator, the Notch intracellular domain, are polyglutamine (pQ)-rich factors that target enhancer elements and interact with other locally bound pQ-rich factors. To understand the functional repertoire of such enhancers, we identify conserved regulatory belts with binding sites for the pQ-rich effectors of both Notch and BMP/Dpp signaling, and the pQ-deficient tissue selectors Apterous (Ap), Scalloped (Sd), and Vestigial (Vg). We find that the densest such binding site cluster in the genome is located in the BMP-inducible *nab* locus, a homolog of the vertebrate transcriptional cofactors *NAB1/NAB2*. We report three major findings. First, we find that this *nab* regulatory belt is a novel enhancer driving dorsal wing margin expression in regions of peak phosphorylated Mad in wing imaginal discs. Second, we show that Ap is developmentally required to license the *nab* dorsal wing margin enhancer (DWME) to read out Notch and Dpp signaling in the dorsal compartment. Third, we find that the *nab* DWME is embedded in a complex of intronic enhancers, including a wing quadrant enhancer, a proximal wing disc enhancer, and a larval brain enhancer. This enhancer complex coordinates global *nab* expression via both tissue-specific activation and interenhancer silencing. We suggest that DWME integration of BMP signaling maintains *nab* expression in proliferating margin descendants that have divided away from Notch–Delta boundary signaling. As such, uniform expression of genes like *nab* and *vestigial* in proliferating compartments would typically require both boundary and nonboundary lineage-specific enhancers.

KEYWORDS developmental genetics; Notch; Su(H); Dpp/BMP; polyglutamine; pQ signal integration; *nab*; imaginal disc patterning; Apterous

NOTCH signaling is a metazoan mechanism that promotes different fates in adjacent cells (Artavanis-Tsakonas 1999; Barad *et al.* 2011; Guruharsha *et al.* 2012). Cell–cell signaling between membrane-bound Notch receptor and its membrane-bound ligands, Delta and Serrate/Jagged, leads to cleavage and nuclear import of the Notch intracellular domain (NICD) (Schroeter *et al.* 1998). In the nucleus, NICD binds the transcription factor (TF) Suppressor of Hairless, Su(H), to activate target genes via Su(H)-bound transcriptional enhancers (Fortini and Artavanis-Tsakonas 1994). This role of Su(H) is further complexified because it can recruit a Hairless repressor complex in the absence of NICD (Bang *et al.* 1995; Barolo *et al.* 2002; Maier *et al.* 2011; Ozdemir *et al.* 2014). This operation is central to diverse developmental contexts including tissue compartment boundaries, where such signaling defines adjacent epithelial domains. For this reason, Notch signaling to an enhancer is frequently integrated with tissue-specific, developmental signaling cues (Voas and Rebay 2004; Ward *et al.* 2006; Liu and Posakony 2012; Housden *et al.* 2014).

Notch-target enhancers can be characterized as either Notch instructive or Notch permissive (Bray and Furriols 2001), although other types are also evident (Janody and Treisman 2011). In the *Drosophila* embryo, the *E(spl)m8* enhancer is a neurogenic target of an instructive Notch signal (Furukawa *et al.* 1995; Lecourtois and Schweisguth 1995; Schweisguth 1995). Ectopic expression of NICD in this context drives *E(spl)m8* expression throughout the dorsoventral (D–V) axis, except in the mesoderm where its enhancer is inhibited by the Snail zinc finger repressor (Cowden and Levine 2002). In contrast, the Notch-target *sim* mesoectodermal enhancer and *rhomboid* (*rho*) neurogenic ectoderm enhancer (NEE) are driven ectopically in a way that is limited by the morphogenic gradient of the Rel-homology domain

doi: 10.1534/genetics.116.186791
Manuscript received January 4, 2016; accepted for publication March 8, 2016; published Early Online March 11, 2016.
Available freely online through the author-supported open access option.
Supplemental material is available online at www.genetics.org/lookup/suppl/doi:10.1534/genetics.116.186791/-/DC1.
[1]Corresponding author: Department of Biology, University of Iowa, 143 Biology Building, 129 E. Jefferson St., Iowa City, IA 52242-1324. E-mail: albert-erives@uiowa.edu

containing factor Dorsal, which cotargets these enhancers (Cowden and Levine 2002; Markstein *et al.* 2004; Crocker *et al.* 2010). Thus, in the context of the *sim* and *rho* enhancers, the Notch signal is only permissive because it is not sufficient for expression.

Wing margin enhancers, which define the border separating the dorsal and ventral compartments of wing imaginal discs, can also receive instructive or permissive Notch signals (Jack *et al.* 1991; Williams *et al.* 1994; Lecourtois and Schweisguth 1995; Neumann and Cohen 1996b). Wing margin enhancers from *E(spl)m8* and *cut* use Notch signaling instructively, whereas enhancers from *vestigial* (*vg*) and *wingless* (*wg*) use the signal permissively (Janody and Treisman 2011). Tellingly, these enhancers respond differently to mutations of genes encoding the Med12 and Med13 subunits of the Mediator coactivator complex, which are required for Notch signaling (Janody and Treisman 2011). In clones with Med12 or Med13 deletions, Notch-instructive margin enhancers from *E(spl)m8* and *cut* fail to drive any expression, while Notch-permissive margin enhancers from *vestigial* (*vg*) and *wingless* (*wg*) drive expression that is limited to cells close to the margin. Thus, diverse developmental enhancers encode contextual information specifying whether the Notch signal is sufficient and therefore instructive or only permissive of activation by other signaling effectors.

How an enhancer integrates Notch signaling with other signaling pathways in a developmental context is an important question. Some insight comes from studies of the nonhomologous, Notch-permissive NEEs at *rho*, *vn*, *brk*, *vnd*, and *sog* (Erives and Levine 2004; Crocker *et al.* 2008, 2010; Crocker and Erives 2013; Brittain *et al.* 2014). These enhancers are driven by the Dorsal morphogenic gradient patterning system of *Drosophila*. Activation is mediated by a pair of linked binding sites for Dorsal and Twist:Daughterless (Twi:Da) heterodimers, as well as by a separate site for the MADF BESS domain containing factor Dip3, which is important for SUMOylation of Dorsal and for Dorsal/Twist cooperativity (Bhaskar *et al.* 2002; Erives and Levine 2004; Ratnaparkhi *et al.* 2008). Notch input is mediated by a Su(H) binding site as shown by overexpression of constitutively active NICD and mutation of the Su(H) site (Markstein *et al.* 2004; Crocker *et al.* 2010). There are also conserved binding sites for the pioneer factor Zelda (Brittain *et al.* 2014), which primes embryonic enhancers (Harrison *et al.* 2011; Nien *et al.* 2011).

Activator sites for Dorsal, Twi:Da, Dip3, and Su(H) exhibit a constrained organization in each NEE (Erives and Levine 2004). Furthermore, Dorsal gradient readouts by NEEs are sensitive to the length of a spacer element that separates the Dorsal and Twi:Da binding sites (Crocker *et al.* 2008, 2010; Crocker and Erives 2013), and which is exploited in the evolutionary tuning of gradient responses (Crocker *et al.* 2008, 2010; Brittain *et al.* 2014). This functional spacer sensitivity of NEEs may involve the polyglutamine (pQ)-enriched *trans*-activation domains of NEE activators: Dorsal, Twi, Da, Su(H), and Zelda (see Figure 1A). Interestingly, Dorsal:Twi coactivation involves the SUMOylation system (Bhaskar *et al.* 2002; Ratnaparkhi *et al.* 2008), which can attenuate pQ-mediated aggregation (Mukherjee *et al.* 2009). The carboxamide side chains of glutamine (Q) and asparagine (N) allow additional hydrogen bonding, which is a key feature of pQ/pN-mediated protein aggregation. Although proteins with pathological expansions of pQ tracts ≥40 residues can self-assemble into cross-β-sheet amyloid fibers (Perutz *et al.* 2002a,b), proteins with shorter pQ tracts can aggregate into complexes when imported into the nucleus and brought together by a DNA scaffold (Perez *et al.* 1998). As such, the lengths of functional *cis*-spacers may modulate the degree of pQ aggregation and/or β-strand interdigitation (Rice *et al.* 2015).

In *Drosophila melanogaster*, the NICD coactivator contains a nearly uninterrupted pQ tract (≥31 residues long) that is conformationally variable and functionally important (Wharton *et al.* 1985; Kelly *et al.* 2007; Rice *et al.* 2015). Many such pQ repeats have been identified in transcriptional activators/coactivators and some have been found to be required for synergistic activation (Wharton *et al.* 1985; Courey and Tjian 1988; Courey *et al.* 1989). Su(H)-bound NICD recruits the pQ-rich Mastermind coactivator (Yedvobnick *et al.* 1988; Newfeld *et al.* 1993; Helms *et al.* 1999; Schuldt and Brand 1999; Kovall 2007), as well as pQ-rich Mediator components (Tóth-Petróczy *et al.* 2008; Janody and Treisman 2011). We hypothesize that Notch-permissive enhancers might function through pQ-aggregated complexes that accumulate in the nucleus. Such enhancer-specific complexes might also continue forming for the duration that these pQ-rich signals are being received such that they constitute a type of *trans*-epigenetic memory. To understand the functional repertoire of Notch-permissive enhancers, we thus seek to identify and study model Notch target enhancers that integrate instructive morphogenic signals via pQ-rich effectors. One candidate pQ/pN-rich effector complex is Mad:Medea, which mediates Decapentaplegic (Dpp)/BMP morphogenic signaling in *Drosophila* (Raftery *et al.* 1995; Hudson *et al.* 1998; Wisotzkey *et al.* 1998). Furthermore, in several of these Dpp/BMP signaling contexts Notch signaling is also active (de Celis 1997; Steneberg *et al.* 1999; Crocker and Erives 2013).

Here we identify and analyze a novel, Su(H)-dependent, Notch/BMP-integrating enhancer in the BMP-inducible gene *nab*, which encodes a conserved transcriptional cofactor (Clements *et al.* 2003; Terriente Félix *et al.* 2007; Ziv *et al.* 2009; Hadar *et al.* 2012). The *nab* enhancer drives expression in two domains abutting the dorsal wing margin and flanking the stripe of Dpp expression in *Drosophila*. We find that this dorsal wing margin enhancer (DWME) is licensed by the selector Apterous (Ap) to read out Notch and BMP/Dpp signaling in the dorsal compartment of wing imaginal discs. Ap is a homeodomain-containing factor specifying the dorsal compartment of wing imaginal discs (Cohen *et al.* 1992; Blair *et al.* 1994). We show that the *nab* DWME, which has multiple Ap-binding sites, is affected by mutations of *ap*. We further find that Nab is required in the dorsal compartment for morphogenetic patterning of both the thorax and wings. We

show that activity of the *nab* DWME is driven by Notch and Dpp signaling through two unpaired Su(H) binding sites and one to three Mad:Medea binding sites and propose that Dpp signaling helps to maintain enhancer activity in off-margin lineal descendants of NICD-positive margin cells. Last, we show that global *nab* expression is driven by the combined activity of the *nab* DWME, a wing pouch quadrant enhancer (QE), a proximal wing enhancer (PWE), and a larval brain enhancer (BrE), all of which function as dual enhancers and silencers. Importantly, we find that some of their Su(H) sites function in interenhancer silencing, revealing another aspect of Su(H)-targeted enhancers.

Materials and Methods

Derivation of binding motifs

Binding motifs follow International Union of Pure and Applied Chemistry (IUPAC) DNA consensus coding and were derived from position-weighted matrices from various datasets as illustrated in Supplemental Material, Figure S1 (also see Table 1). The Mad:Medea binding motif 5′-CNBYGDCGYSNV is a consensus IUPAC motif that we derived from embryonic ChIP-chip data (Bergman *et al.* 2005) available on JASPAR (Sandelin *et al.* 2004; Mathelier *et al.* 2015). The Zelda binding motifs, 5′-CAGGYAR, 5′-CAGGTAV, and 5′-YAGGTAR, were based on previously published characterization of Zelda ChIP-chip data (Harrison *et al.* 2011; Nien *et al.* 2011). The Apterous binding motif 5′-RYTAATKA is a consensus IUPAC motif, which we derived from bacterial one-hybrid (B1H) data from the FlyFactorSurvey project (Zhu *et al.* 2011). We also derived the Pangolin (dTcf) binding motif 5′-TTTGWWS from B1H data available from the FlyFactorSurvey. For the Scalloped dimer binding motif, which is necessary for recruitment of Vestigial, we realigned the known binding sites from the *cut*, *sal*, and *kni* enhancers (Halder and Carroll 2001) and found we could derive the tighter consensus 5′-RVATTNNNNRVATH by using the reverse complement sequences of some sites in a consensus alignment (see Figure S1). Sequences containing the above sites were identified from the 1344 conserved regulatory belts (*i.e.*, clusters of nonprotein-coding conservation peaks) containing sites matching the Su(H) motif 5′-YGTGRGAAH. Motifs were searched using regular expression pattern matching, perl, and grep commands in a UNIX shell environment.

Molecular cloning

DNA fragments were amplified from either genomic DNA extracted from w^{1118} flies (DNA → *nab-C*, and DNA → *nab-A* → *nab-Ax*), or DNA prepared from the Berkeley *Drosophila* Genome Project (BDGP) BAC clone BACR48M07 and its subcloned derivatives (BAC → *nab-CDAB* → *nab-AB* → *nab-B*, *nab-CDAB* → *nab-DAB* → *nab-DA*, and BAC → *nab-CDA*). All enhancer fragments were sequenced in both directions to confirm identity of clones and the absence of unwanted mutations, although the larger fragments were not necessarily sequenced through their entire lengths (see File S1 and File S2). Mutations of individual Su(H) sites were created using two-step PCR-mediated stitch mutagenesis to introduce changes as indicated in the text and sequenced to confirm these mutations. Triple mutation of the Mad:Medea binding sequences in the *nab-A* fragment was synthesized using gBlock synthesis (Integrated DNA Technologies) of the cloned *nab-A* fragment sequence in which the prominent 5′-CG dinucleotide of each site was replaced with a 5′-TT dinucleotide (see Figure S1). Outside of the introduced mutations, the sequences obtained for mutagenized clones are otherwise identical to their parent clones (*nab-A*, *nab-AB*, or *nab-CDA*). To sequence inserts cloned into the pH-Stinger vector, we used Stinger-fwd: (5′-ATA CCA TTT AGC CGA TCA ATT GTG C) and Stinger-rev: (5′-CTG AAC TTG TGG CCG TTT ACG).

Amplified *nab* intronic fragments were cloned into the *Xba*I site of the pH-Stinger vector (TATA-box containing *hsp70* core promoter driving nuclear eGFP) (Barolo *et al.* 2004). The *nab-A* fragment was also cloned into the *Eco*RI site of the "−42 *eve-lacZ*" pCaSpeR vector. The *nab* intronic fragments were amplified using a high-fidelity *Taq* polymerase (NEB Platinum Taq mix) and the following oligonucleotide primer pairs designed from the reference iso-1 assembly: *nab-A*: A-fwd (5′-TGGACGCAACTGGTCTGATA) and A-rev (5′-GACCAAGGATGCGATACGAT); *nab-B*: B-fwd (5′-TTTCA GAAGGGGTTGAACC) and B-rev (5′-CGTATGCATAAGAAAC TGGC); *nab-C*: C-fwd (5′-ACAAGTACAATGGACATGG) and C-rev (5′-GAAAAGATACATATGAGTAATGC); *nab-Ax*: A-fwd and Ax-rev (5′-CCAGCAAGGATTGCCAGG); *nab-AB*: A-fwd and B-rev; *nab-DA*: D-fwd (5′-CTCATATGTATCTTTTC, which spans reverse complement of C-rev) and A-rev; *nab-DAB*: D-fwd and B-rev; *nab-CDA*: C-fwd and A-rev; and *nab-CDAB*: C-fwd and B-rev. All primers included flanking restriction sites for *Xba*I (5′-TCTCAGA) or *Bsa*I/*Eco*RI (5′-GGTCTCGAATTC).

Dissection and antibody staining

Wandering third instar larvae were dissected and fixed with 11.1% formaldehyde in PBS for 30 min. Tissue was washed for 30 min in PBT and then blocked with 1% BSA in PBT for 1 hr. Tissue was incubated with primary antibodies overnight and with secondary antibodies for 1.5 hr. After each antibody incubation, a series of washes was done for 30 min. Nuclear stained tissue was incubated with 17.5 μM DAPI in PBT for 5 min and then washed for 30 min. Subsequently the imaginal discs or larval brains were dissected from the remaining tissue and cuticle. This dissection was done on a slide in 80% glycerol. The slide was then covered with a supported coverslip and imaged with a confocal microscope.

The following primary antibodies were used: chicken anti-GFP (1:250) (Abcam: ab13070), rabbit anti-Gal4 (1:250) (Santa Cruz Biotechnology: sc-577) mouse anti-Wg (1:25), mouse anti-Ptc (1:50), mouse anti-En (1:50), and mouse anti-β-galactosidase/40-1a (1:12). The last four monoclonal antibodies were developed by S. M. Cohen, I. Guerrero, C. Goodman, and J. R. Sanes, respectively, and were obtained

Table 1 Regulatory belts with sites for pQ-rich effectors of Notch/BMP signaling and pQ-deficient wing disc selectors

Filtering step	Parameter	Output
Unique *D. mel*. belts with Su(H) site(s)[a]	5′-YGTGRGAAH	1344 belts[b]
+ChIP-chip pMad binding motif[c]	5′-CNBYGDCGYSNV	221 belts
+ChIP-seq Zelda binding motif[d]	5′-CAGGYAR, 5′-CAGGTAV, or 5′-YAGGTAR	98 belts
+B1H Apterous binding motif[e]	5′-RYTAATKA	31 belts
+Sd:Sd:Vg *in vivo* binding consensus[f]	5′-RVATTNNNNRVATH	13 belts
−Tcf/Pangolin *in vivo* consensus[g]	Missing: 5′-TTTGWWS	2 belts (*nab* intronic, *cv-c* intergenic)
+homotypic site clustering[h]	≥2 Su(H) sites, or	1 belt (*nab* intronic)
	≥3 Mad sites, or	1 belt (*nab* intronic)
	≥2 Zld sites, or	1 belt (*nab* intronic)
	≥2 Ap sites	1 belt (*nab* intronic)

[a] Many *D. melanogaster* belts map to two or more discontinuous *D. virilis* blocks, which were either spaced far apart in the *D. virilis* assembly or else were present in separate contigs.
[b] These are composed of 1157 belts with a single Su(H) site, 158 belts with two sites, and 29 belts with 3–5 clustered sites.
[c] IUPAC developed from reported ChIP-chip profile (Bergman *et al.* 2005).
[d] IUPAC developed from reported embryonic ChIP-chip profile (Harrison *et al.* 2011).
[e] Bacterial one-hybrid assay (Noyes *et al.* 2008).
[f] Consensus matches known Sd:Sd:Vg regulatory binding sites at *cut*, *sal*, and *kni* enhancers (Halder and Carroll 2001).
[g] Tcf is a pQ-deficient transcriptional effector of Wg/Wnt signaling. Motif is based on ChIP-chip data (van de Wetering *et al.* 1997) and *in vivo* consensus (Archbold *et al.* 2014).
[h] A comparison of the regulatory belts at *nab* and *cv-c*.

as concentrates/supernatants from the Developmental Studies Hybridoma Bank, created by the National Institute of Child Health and Human Development (NICHD) of the NIH and maintained by the University of Iowa. Primary antibodies were detected with Cy2-conjugated goat antichicken (1:1000) (Abcam: ab6960), Cy3-conjugated goat antirabbit (1:1000) (Abcam: ab6939), or Cy5-conjugated goat antimouse (1:1000) (Invitrogen: A10525) secondary antibodies.

Drosophila stocks and crosses

Functional analysis of *nab* and the *nab* DMWE were performed using stocks obtained from the Bloomington and Kyoto stock centers and the Vienna *Drosophila* RNAi Center (VDRC). The following stocks from the Bloomington *Drosophila* Stock Center were used: N^1 (6873), ap^{GAL4} (3041), en^{GAL4} *UAS:Dcr* (25753), *UAS:GFP* (6874), and the 3-kb *dpp-lacZ* reporter line (8404). The *nab*-RNAi (1607) stock was obtained from the VDRC. The following *nab* enhancer trap stocks were obtained from the Kyoto Stock Center: nab-NP1316 (112622) and nab-NP3537 (104533).

For the mutant Notch experiments, virgin N^1/*FM7c* flies were crossed with X-linked *nab-A-Hsp70-GFP* (DWME pH-Stinger reporter) males. An overnight collection of F_1 embryos from this cross was then sorted into two populations based on the presence or absence of GFP expression, which would indicate the presence of the *FM7c* balancer, which carries *twist:GAL4 UAS:GFP*. Again at 12 and 24 hr postcollection, a few newly GFP-positive embryos were removed from the initially GFP-negative population. These two populations of sorted embryos (±GFP) were then grown to the wandering third instar stage and dissected and stained as described.

For the mutant Apterous experiments, virgin ap^{GAL4}/*CyO* females were crossed with X-linked *nab-A-GFP* males. Virgin F_1 females without *CyO* were then crossed with ap^{GAL4}/*CyO* males. F_2 larvae with background salivary gland GFP expression, indicating presence of the pH-Stinger vector (Zhu and Halfon 2007), were then dissected and stained.

Data availability

Transgenic lines carrying all *nab* enhancer reporters described in this study are available upon request.

File S1 is a text file containing FASTA sequences for the entire *nab-CDAB* enhancer complex (reference iso-1 genome) as well as the cloned *nab-A* sequence. Annotated sequences for the cloned *nab*-A fragment and the *nab*-CDAB enhancer complex have also been deposited at GenBank under the accession numbers KU375573 and KU375574, respectively. File S2 is a pdf file showing an annotated alignment of all cloned sequences relative to the reference genome. Figure S1 shows our derivation of IUPAC transcription factor motifs that we used in this study. Figure S2 shows images of *nab* DWME-driven GFP expression in live larvae and pupae and in live dissected imaginal discs. Figure S3 shows overnight beta-gal staining of wing discs dissected from all seven independent *P*-element lines that we established for the *nab-A* (DWME) *lacZ* reporters. Figure S4 shows how *nab* DWME binding sites relate to (default) fixed nucleosome positions inferred from embryonic data from Langley *et al.* (2014).

Results

Identification of conserved regulatory belts with binding sites for Notch/BMP effectors and wing disc selectors

The Su(H) binding motif (5′-YGTGRGAAH) is remarkably constant across bilaterians and unique to Su(H) (Tun *et al.* 1994). To identify novel enhancers integrating Notch signaling with pQ-rich morphogenic effectors akin to the NEEs, we first developed a computational pipeline that identified 1344

evolutionarily conserved regulatory belts containing one or more adjacent Su(H)-binding sites (pipeline and other identified enhancers will be described in a separate article). By "regulatory belt" we mean a characteristic cluster of nonprotein coding conservation peaks consistent with a regulatory module (*e.g.*, enhancer, insulator, and core promoter). We find that most regulatory belts span a range of 15–25 peaks of genus-wide conservation. Each such peak typically corresponds to one to three overlapping binding sites for TFs. This is consistent with enhancers requiring multiple *cis*-elements for both nuanced activity patterns and restricted tissue specificity. Here, we use these candidate Su(H)-targeted genetic elements to find a model enhancer that is well suited for testing hypotheses about functional enhancer grammar.

To find enhancers that are integrating both Notch and Dpp/BMP signaling, we searched for the subset of 1344 *D. melanogaster* regulatory belts that also contain a binding site for the pQ/pN-rich Mad:Medea complex, which mediates activation of Dpp/BMP targets (Sekelsky *et al.* 1995; Newfeld *et al.* 1996, 1997; Wiersdorff *et al.* 1996; Hudson *et al.* 1998; Wisotzkey *et al.* 1998; Campbell and Tomlinson 1999; O'Connor *et al.* 2006; Weiss *et al.* 2010). Specifically, we developed and searched for the subset of belts containing the IUPAC consensus motif that we derived for phosphorylated-Mad (pMad) ChIP-seq peaks (see *Materials and Methods* and Table 1). We also searched for sequences targeted by Zelda, which is a pQ-rich pioneer factor for embryonic enhancers that is also expressed in wing imaginal discs (Staudt *et al.* 2006; Harrison *et al.* 2011). Altogether, we found 98 unique regulatory belts containing binding sites for this pQ-rich set of activators Su(H), pMad:Medea, and Zelda (Table 1 and Figure 1).

To find enhancers that are specific to the wing imaginal disc, we refined the subset of 98 down to those that also had binding sites for three wing imaginal disc selectors: (i) Apterous (Ap), which is expressed throughout the dorsal wing compartment (Cohen *et al.* 1992), and (ii) Scalloped (Sd) and Vestigial (Vg), which are expressed at the dorsal/ventral compartment boundary where there is active Notch–Delta signaling (Halder *et al.* 1998; Halder and Carroll 2001; Koelzer and Klein 2006). By definition, selectors are TFs that are responsible for a stable binary cell fate decision (García-Bellido 1975; Lawrence *et al.* 1979; Akam 1998). For Ap, we derived the IUPAC consensus motif 5′-VYTAATKA from its DNA binding profile and found 31/98 regulatory belts with sequences matching this motif (Table 1). For Sd and Vg, we found that 13 of these 31 regulatory belts contain the canonical Sd dimer binding site that recruits the Sd:Sd:Vg complex (Table 1) (Halder and Carroll 2001). All three selectors (Ap, Sd, and Vg) are deficient in pQ/pN tracts unlike the graded signal-dependent effectors (*e.g.*, see Figure 1), Mediator coactivators subunits, and TATA binding protein (TBP).

Finally, to focus on pQ-rich graded signal integration of just the Notch and BMP pathways, we set aside 11 of the 13 regulatory belts that had potential binding sites for Tcf/Pangolin. Tcf/Pangolin mediates transcriptional activation in the Wnt and β-catenin/Armadillo signaling pathway (van de Wetering *et al.* 1997; Archbold *et al.* 2014). This last filtering step left us with two regulatory belts at the *nab* and *crossveinless c* (*cv-c*) loci, which are located on the left and right arms of chromosome three, respectively. The gene *nab* encodes a BMP-induced transcriptional cofactor involved in embryonic and imaginal disc development (Clements *et al.* 2003; Terriente Félix *et al.* 2007; Ziv *et al.* 2009; Hadar *et al.* 2012), while the gene *cv-c* encodes a BMP-induced Rho-type GTPase activating protein (RhoGAP) involved in cross-vein morphogenesis (Matsuda *et al.* 2013). We later describe how RNAi knockdown of *nab* phenocopies *crossveinless*-type wings, suggesting both *nab* and *cv-c* function in a common developmental genetic pathway. In this study, we focus on the *nab* regulatory belt and its interactions with adjacent regulatory elements because it has more sites for each factor than the *cv-c* regulatory belt (Table 1).

The nab DWME drives D–V wing margin expression modulated along the anterior–posterior axis

The dense site cluster overlying the *nab* regulatory belt is located in the long first intron of *nab* in *Drosophila* (thick bar underline in Figure 2A). This same belt is part of a smaller 2.7-kb intronic fragment containing several regulatory belts conserved in both *D. melanogaster* and *D. virilis* (see boxed region in Figure 2A). We cloned the predicted 764-bp *nab-A* fragment and found it corresponds to a DWME with augmented expression in regions corresponding to peak pMad levels (Figure 2, B–L). (Note: this fragment is 764 bp long in the reference iso-1 genome, but is 762 bp long in the cloned fragment due to polymorphic indels in two separate poly-A tracts.) The *nab-A* fragment was tested using two different core promoters with different reporter transgenes: (i) a 270-bp minimal *hsp70* core promoter–eGFP–nls fusion, and (ii) a 205-bp minimal *eve* core promoter–*lacZ* fusion (Figure 2C). These constructs also tested the *nab-A* enhancer fragment in both orientations relative to these core promoters (Figure 2, B and C). We generated seven and five independent *P*-element integrations of the *lacZ* and *eGFP–nls* reporter constructs, respectively, and found all 12 to drive the same expression pattern.

We find that the *nab-A* fragment works equally well across these different reporter constructs in live dissected and undissected discs (Figure S2), in fixed and double-stained imaginal discs (Figure 2, D–J), in fixed discs stained for β-gal expression (Figure 2K and Figure S3), and in fixed discs incubated with an antisense *lacZ* RNA probe (Figure 2L). *In situ* hybridization with the same antisense *lacZ* RNA probe also shows that the *nab-A* fragment drives expression in stage 9/10 long germ-band-extended embryos in what may be a subset of embryonic neuroblasts, a known site of *nab* expression (Clements *et al.* 2003).

In the wing imaginal disc, the *nab* DWME drives expression from the D–V border region and into the dorsal compartment by several cells but only in two spots roughly centered in the anterior and posterior compartments. These spots occur in

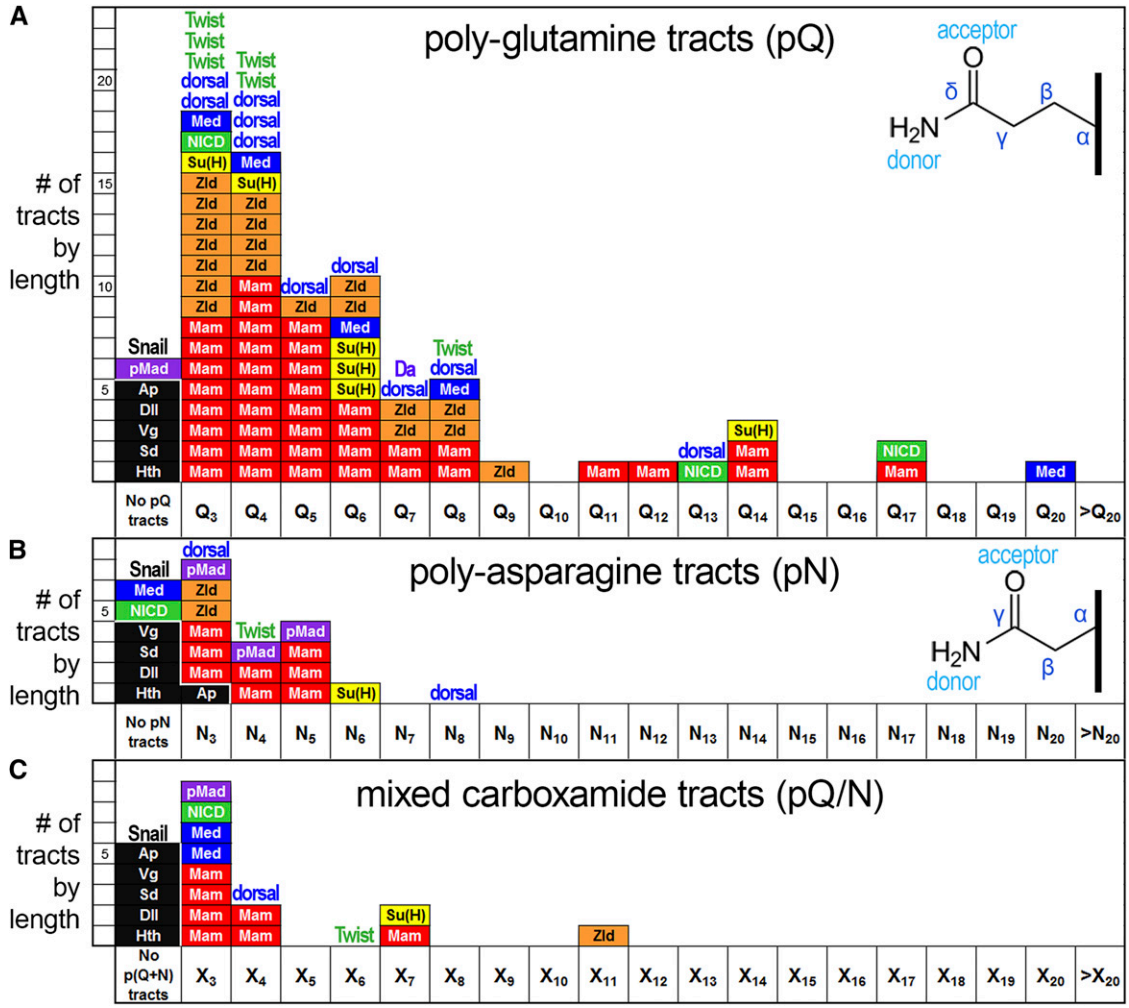

Figure 1 Consideration of the polyglutamine (pQ) and polyasparagine (pN) content of factors in computational genomic searches for novel Notch-signal integrating enhancers. (A) Histogram of pQ tracts for the Dpp effectors, pMad (violet) and Medea (Med, blue); the Notch effectors, Su(H) (yellow) and its coactivators, the Notch intracellular domain (NICD, green) and Mastermind (Mam, red); and the temporal patterning factor Zelda (Zld, orange). Binding sites for these factors are enriched in the *nab* DWME. Also shown is the pQ content for activating TFs targeting the analogous NEEs: dorsal, Twist, Daughterless (Da), Zld, and Su(H). Snail (Sna) is a NEE-targeting transcriptional repressor and is devoid of pQ content. Each pQ tract, defined as a contiguous sequence of Qs ≥ 3, is represented by a single box in a bin corresponding to its length. In contrast to the patterning factors, the selector DNA binding factors (Ap, Dll, Sd, and Hth) and cofactors (Vg) are devoid of pQ tracts, likely indicating distinct modes of regulation separate from the signaling pathway effectors (see text). Similar trends are also seen with pN (B) or with mixed polycarboxamide (X) tracts (C).

regions with peak pMad levels as previously shown (Tanimoto *et al.* 2000; Restrepo *et al.* 2014). The *nab* DWME also drives expression in a highly stereotyped pattern that is unique to each compartment. In addition to the thin interrupted row of expression along the D–V margin, expression occurs as an elongated anterior spot and a broader mitten-shaped posterior spot abutting the margin (*e.g.*, compare anterior and posterior spots on the left and right sides of each disc in Figure 2K). This robust DWME-driven expression pattern is consistent with our desired goal of finding a wing disc compartment-specific enhancer integrating two orthogonal developmental signals: (i) a D–V Notch margin signal and (ii) a graded anterior–posterior (A–P) BMP morphogenic signal. Because endogenous *nab* is expressed in a broader wing pouch pattern than what we observe for the *DWME*-driven reporters, below we address how the DWME relates to other possible enhancers at *nab*. We also address how some of the predicted sites contribute to DWME activity and how the DWME contributes to Nab function in wing development.

The first intron of nab harbors four separate enhancers

To understand the role of the *nab* DWME activity in the overall *nab* expression pattern, we made a series of constructs containing various intronic fragments that we cloned from the first intron of the *nab* locus (Figure 3A). These were tested by anti-GFP antibody staining of dissected larval tissues from independent *P*-element integrated lines as well as pools of these lines (see *Materials and Methods*). Consistent with the presence of insulators in the pH-Stinger vector,

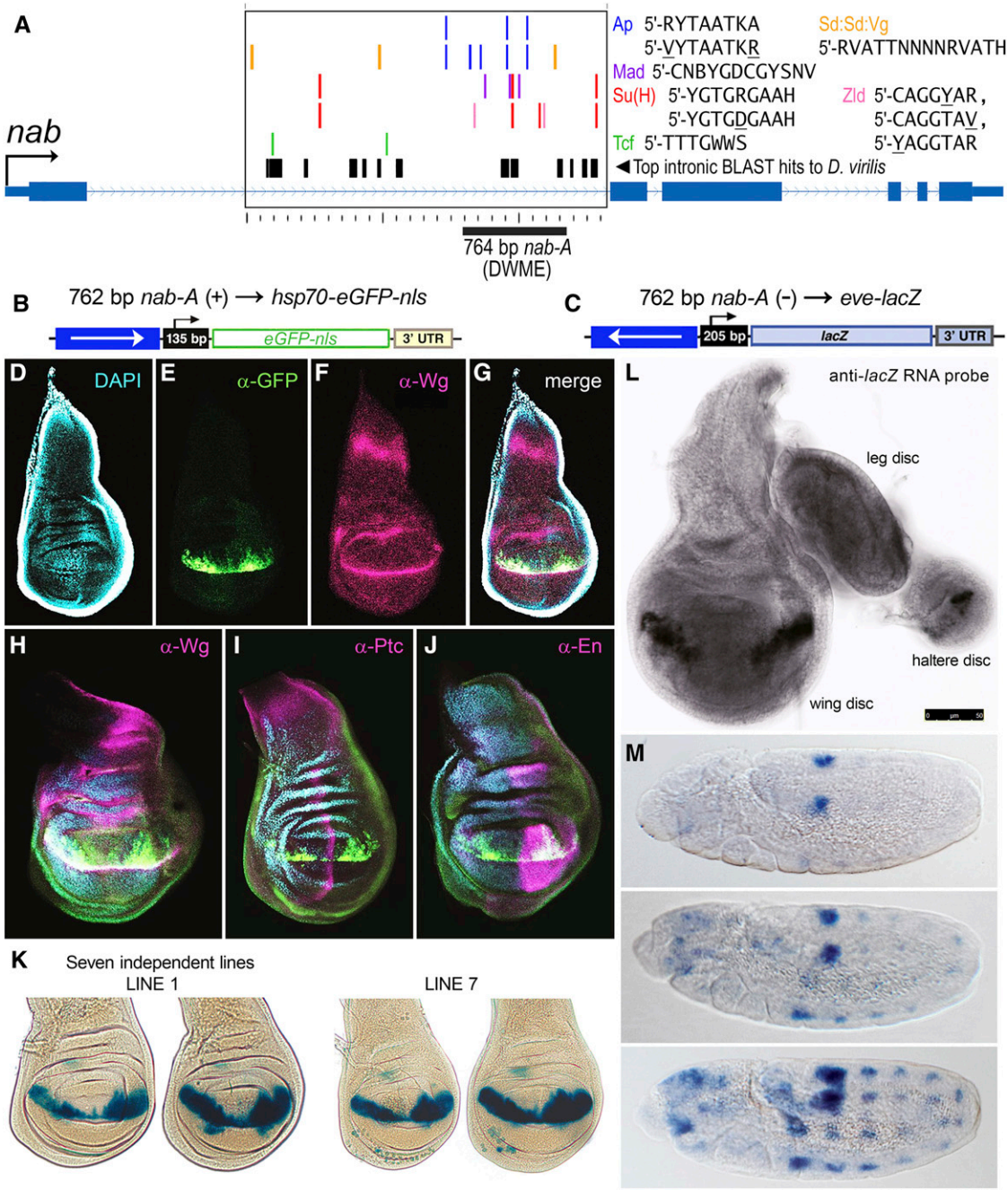

Figure 2 A highly conserved regulatory block in the *Drosophila nab* locus is a robust dorsal wing margin enhancer (DWME). (A) Diagram of the *nab* locus from *D. melanogaster* showing sites matching binding motifs (color-coded boxes on separate tracks in large intronic box) within a 2.7-kb intronic block that contains several regulatory belts conserved across the genus. We cloned a predicted 764-bp region, the *nab-A* fragment (thick bold underline), for having one of the highest concentrations of sites for Su(H), Mad, Zelda, Apterous (Ap), and the Scalloped (Sd) and Vestigial (Vg) complex (Sd:Sd:Vg) without having any Tcf sites. (B and C) We cloned the *nab-A* fragment in front of two core promoter reporter genes: an *hsp70* core promoter fused to an eGFP-nls reporter gene in a gypsy insulated construct (B), and an *eve* core promoter fused to the *lacZ* reporter gene (C). Independent *P*-element transgenic lines with each reporter cassette gave identical expression patterns despite differences in integration sites, core promoters, and enhancer orientation relative to the core promoter (arrows in enhancer box, and + or − signs in parentheses). The cloned 762-bp fragment is 2 bp shorter than the reference sequence due to single base pair contraction polymorphisms in two separate poly-A runs. (D–F) Expression from the *nab-A* (DWME) EGFP reporter along the dorsal wing margin. Different color channels indicate DAPI (D, cyan); GFP (E, green); and Wingless (Wg) (F, magenta), which mark the D–V compartment margin, a ring around the wing pouch, and a broad stripe across the proximal part of the wing disc. (G) Merged images of D–F. (H–J) Additional discs double-labeled with antibodies to Wg (H), and Ptc (I), and En (J), which mark the A–P margin and posterior compartment, respectively. The anterior DWME expression pattern is characteristically longer than the posterior compartment side, which in turn stretches deeper into the dorsal compartment than the anterior compartment expression pattern. (K–M) DWME-driven *lacZ* reporter activity in late third instar discs (K and L) or in germ-band extended embryos (M). DWME-driven expression was detected with overnight X-gal staining (K) or with a digU-labeled antisense *lacZ* RNA probe (L and M). Both wing (K and L) and haltere (L) discs show the characteristic twin spots of DWME-driven activity, while the embryonic expression is detected in a subset of lateral neuroblasts.

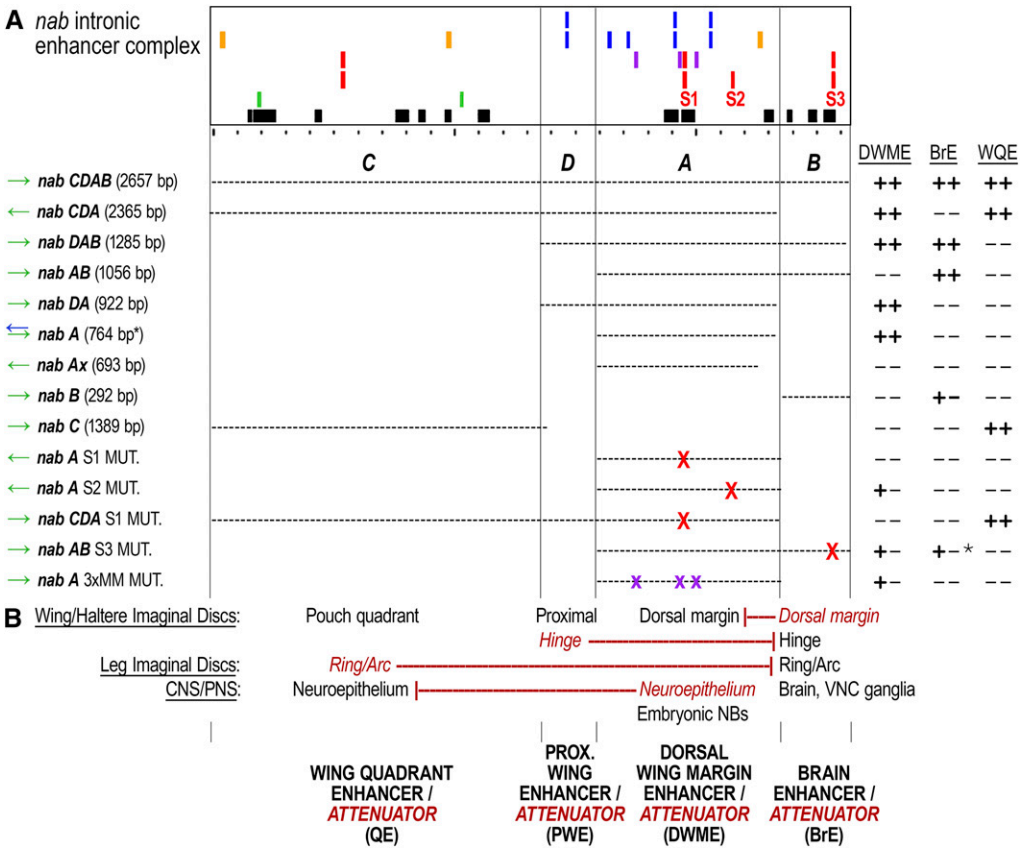

Figure 3 The *Drosophila nab* harbors several regulatory modules functioning as both enhancers and mutual silencers/attenuators. (A) We cloned and tested the indicated series of *nab* intronic fragments to understand the regulatory logic of *nab*'s expression in wing imaginal discs. The colored boxes follow the key in Figure 2 except Zelda sites are not shown for clarity. To refer to the different enhancers we identified, we defined four different intronic regions as the *nab-C*, *nab-D*, *nab-A* (DWME), and *nab-B* fragments. We also labeled the four best matches to Su(H) binding motifs (sites S1–S3) and mutated these sites in the indicated constructs (S1, S2, or S3 MUT and Xs in construct). These regions can be understood as having four major enhancer activities: the dorsal wing margin enhancer (DWME); a larval brain enhancer (BrE), which drives dense expression in neuronal lineages; a wing imaginal disc quadrant enhancer (QE), which complements the DWME activity to match the endogenous expression pattern; and a proximal wing enhancer (PWE). ++ indicates strong expression, + indicates weak expression, while maintaining the indicated pattern. * means there is a more nuanced description of the expression in the main text. Both the sizes and the direction of the cloned insert relative to the core promoter are shown for each construct. (B) Each cloned enhancer was found to drive a distinct expression activity associated with the endogenous *nab* locus, a distinct ectopic activity, or expression level that was not associated with the endogenous *nab* locus, and a distinct silencing or attenuation activity acting on ectopic expression patterns and levels (red repression symbols connecting one silencer/attenuation activity in one enhancer to the ectopic activity/level in another intronic enhancer).

independent lines of the same construct recapitulated each other's expression patterns.

After comparing a PGawB *nab GAL4* enhancer trap line (*nab*^{NP1316}, insertion site 48 bp upstream) (Hayashi *et al.* 2002) with the various constructed transgenic reporter lines, we discovered that we identified separate enhancer activities for all known tissues in which *nab* is expressed (Figure 4A *vs.* Figure 4, B–I). The expression pattern of the endogenous *nab* locus in late third instar wing imaginal discs (Figure 4A) is driven by a combination of (i) the DWME activity from the 764-bp *nab-A* fragment (Figure 4B), (ii) QE activity from a 1.4-kb *nab-C* fragment (Figure 4C), and (iii) PWE activity from the combined 2.4-kb *nab-CDA* fragment (triple arrows pointing to dispersed expression pattern in Figure 4D). The PWE activity, which we also find in both the endogenous enhancer trap line (see triple arrows in Figure 4A) and a larger 2.7-kb *nab-CDAB* fragment (Figure 4E), likely requires elements present in both *nab-C* and *nab-D* fragments because neither the *nab-C* (Figure 4C) nor the *nab-DA* fragment (Figure 4H) recapitulates this pattern on its own.

The robust expression of the endogenous enhancer trap reporter in the dorsal margin of the wing pouch (single horizontal arrow in Figure 4A) is recapitulated in all reporter lines carrying the *nab-A* fragment (Figure 4B and single horizontal arrows in Figure 4, D and E) with one exception summarized in the next section. Furthermore, this dorsal margin activity is absent in the *nab-C* fragment, which only drives a quadrant pattern in wing imaginal discs (see hollow arrow pointing to gap of expression at margin in Figure 4C). The combined *nab* QE + DWME expression pattern, which we see in the *nab-CDA* and *nab-CDAB* reporters and the *nab*^{NP1316} P{GawB} enhancer trap (Figure 4, A, D, and E), is also recapitulated by a second P{GawB} enhancer trap (*nab*^{NP3537}, data not shown), which has an insertion site 1 bp upstream of *nab* but in the opposite orientation as *nab*^{NP1316}, and a third, previously characterized P{GabB} *nab* enhancer trap line, S149, which has a reported insertion site 23 bp upstream (Gerlitz *et al.* 2002; Ziv *et al.* 2009; Hadar *et al.* 2012).

We also observed that all *nab* enhancer fragments driving wing pouch expression patterns (DWME and QE) also did so in the haltere imaginal discs ("h" discs in single prime lettered panels of Figure 4). This suggests to us that *nab* may play a role in both wing and haltere development. This could indicate that this function predates evolution of haltere balancing organs from wing discs in dipteran ancestors (Lewis 1978; Weatherbee *et al.* 1999).

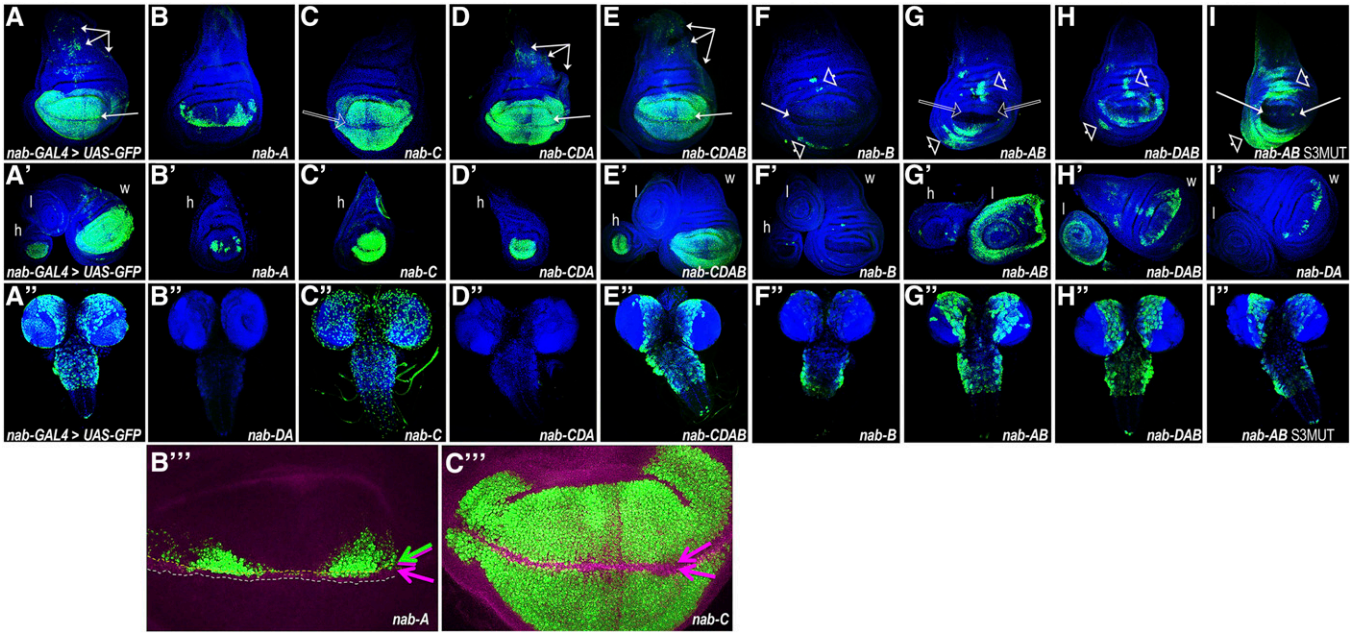

Figure 4 Activities of dissected regulatory modules from the *nab* intronic enhancer/silencer complex. (A–I) GFP reporter expression driven by *nab-GAL4>UAS-eGFP* (A) or by different *nab* enhancer modules driving *eGFP-nls* (B–I). The first row depicts third instar wing imaginal discs; the middle row (single prime) depicts additional third instar discs labeled for halteres (h), leg (l), and wing (w) discs; and the third row (double prime) depicts expression patterns in third instar larval brains, if any. (A–I) The endogenous *nab* expression pattern in wing imaginal discs (A) appears to be the result of discrete activities from: the *nab-A* fragment, which contains the dorsal wing margin enhancer (B); the *nab-C* fragment, which contains a wing pouch/quadrant enhancer (C); a nondescript proximal wing disc enhancer seen with most intronic fragments containing the *nab-D* region (triple arrows in D and E); and the *nab-B* fragment, which contains a hinge enhancer that functions in the absence of the *nab-C* fragment (arrowheads in F–I). Note that the *nab-C* fragment is missing expression at the margin and has more uniform levels of expression throughout the pouch relative to either the *nab-GAL4* enhancer trap (A) or fragments containing both the *nab-C* and *nab-A* regions (empty arrow in C). (A′–I′) Fragments with activities from both the *nab-A* and *nab-C* fragments recapitulate in endogenous *nab* expression in the haltere disc. (A′′–I′′) Most of the endogenous expression of *nab* in the larval brain and ventral nerve cord (A′′) is recapitulated by *nab* intronic fragments carrying the *nab-B* fragment (E′′–H′′) but it is noticeably weaker by itself (F′′). This pattern corresponds to dense expression in neuronal lineages and four cells in the posterior tip of the ventral nerve cord. The *nab-C* fragment has ectopic brain activity that is completely silenced by activities present in the *nab-DA* fragment (see entire brain in D′′ and optic lobes and posterior ventral nerve cord regions in E′′). The *nab-AB* fragment also drives a strong ectopic leg disc ring pattern (see G′ and H′) that is repressed in the presence of the *nab-C* fragment (see E′). Similarly, the dorsal wing margin activity of *nab-A* (B) is silenced in the presence of *nab-B* (see empty arrows pointing to margin in *nab-AB* disc in G) except when *nab-D* is also present (see *nab-DAB* disc in H). The S3 Su(H) binding site in *nab-B* appears to mediate repression of the wing hinge activity inherent to *nab-B* and the dorsal wing margin activity inherent to *nab-A* because there is augmentation of both of these patterns in the *nab-AB* S3 mutated construct (I, arrows point to twin spots along the dorsal margin of the compartment boundary, and arrowheads point to expanded hinge pattern). This same site is not absolutely required for the *nab-B* brain activity (I′′). Neither the *nab-DA* nor the *nab-A* are able to drive any brain expression (representative blank *nab-DA* disc is shown in B′′), strongly suggesting that the *nab-B* fragment is necessary and sufficient for the overall gross expression pattern of *nab* in the brain. (B′′′ and C′′′) Shown are blown-up images of the *nab-A* and *nab-C* activities in the wing disc (green) double labeled for Wg (magenta).

The endogenous enhancer trap reporter is expressed in entire neuronal lineages of the larval brain and in four distinct neurons/cells at the posterior tip of the ventral nerve cord (Figure 4A′′). We find that a 292-bp *nab-B* fragment, located immediately downstream of *nab-A* (Figure 3A), drives the same pattern but at lower levels than the endogenous locus (Figure 4F′′). These lower levels of expression are rescued by larger fragments containing the *nab-B* region: *nab-AB* (Figure 4G′′), *nab-DAB* (Figure 4H′′), or *nab-CDAB* (Figure 4E′′) fragments. This suggests that the minimalized larval BrE present in the *nab-B* fragment normally functions with additional elements that span into the adjacent *nab-A* fragment. Nonetheless, a 693-bp truncated *nab-A* fragment (see *nab-Ax* fragment in Figure 3A), which is missing a conserved sequence that is present on the side flanking the *nab-B* fragment, does not drive any detectable activity in either imaginal discs or larval brain (data not shown). This might signify that the conserved block present in *nab-A* and separating it from the *nab-B* fragment is required for both the DWME and BrE activities. Alternatively, BrE boosting elements may be located elsewhere in the *nab-A* fragment.

The nab enhancers also function as mutual silencers

For each of the four distinct and separable enhancer activities in the first intron of *nab*, we also find distinct silencer activities (Figure 3B). For example, while the *nab-C* fragment does not recapitulate the larval BrE activity, it does drive ectopic expression in a more superficial set of larval brain cells, possibly neuroepithelial cells or glia, and some distinct neurons in the ventral nerve cord (Figure 4C′′). This ectopic activity

associated with *nab-C* is not seen from the endogenous locus (Figure 4A′′) or from any fragment that also contains the *nab-DA* region (Figure 4, D′′ and E′′). This suggests that the ectopic larval brain activity endowed by *nab-C* is silenced by elements present in *nab-DA* (Figure 3B).

In a second example, we find that the *nab-AB* enhancer is a potent ring enhancer in leg imaginal discs ("l" disc in Figure 4G′), which is an activity that is not seen for the *nab* enhancer trap reporter (l disc in Figure 4A′). This activity is attenuated (*i.e.*, made less robust) in the *nab-DAB* fragment (l disc in Figure 4H′) and is completely silenced in the larger *nab-CDAB* fragment. This suggests that the ectopic leg disc activity endowed by *nab-AB* is silenced by elements spanning *nab-C* and *nab-D* (Figure 3B).

In yet a third example, which we previously mentioned as an exception to the presence of DWME activity in all fragments containing *nab-A*, we find that the *nab-AB* fragment obliterates dorsal wing margin expression (arrows in Figure 4G). However, this same silencing activity is only able to attenuate the DWME in the context of the larger *nab-DAB* fragment (Figure 4, H and "w" disc in H′). These results suggest that the *nab-B* fragment is simultaneously a larval brain enhancer and a dorsal wing margin silencer/attenuator. In a related fourth example, the *nab-D* fragment also appears to modulate and attenuate *nab-A*'s DWME activity in the context of the *nab-DA* fragment (Figure 4I′).

A fifth example of dual enhancer/silencer activity is intertwined with the above third example of the BrE's wing disc silencing activity. The *nab-AB* fragment drives ectopic expression in the wing imaginal disc hinge region near the stripe of peak Dpp (arrowheads in Figure 4G). This activity is attenuated in the *nab-DAB* fragment (see arrowheads in Figure 4, H and "w" disc in H′) and completely silenced in the *nab-CDAB* fragment (Figure 4E).

Thus, we find that all of the distinct *nab* enhancer fragments possess both endogenous (*i.e.*, *nab*-related) enhancer activities and ectopic enhancer activities. However, these same enhancers also function as interenhancer silencers of ectoptic activities and attenuators that modulate their nonectopic activities. These activities are summarized in Figure 3B. Later, we describe finding that at least one of the intronic Su(H) binding sites involved in inducible activation is also involved in interenhancer silencing and attenuation.

Activity of nab DWME requires Notch signaling and Su(H) sites

Single nucleotide transversions to any of the core positions in the invariant Su(H) binding sequence, 5′-YGTGRGAA (core positions underlined), are sufficient to eliminate binding *in vitro* (Tun *et al.* 1994). Therefore, to verify that the *nab* DWME is targeted by Notch signaling via its two separate (unpaired), canonical Su(H) binding sites, we compared DWME activity from *nab-A* fragments containing either wild type Su(H) sites, a mutated S1 site, or a mutated S2 site (Figure 5, A–E).

The central S1 site is the only sequence within the *nab-A* fragment that matches the motif 5′-YGTGRGAAH, which we used in our computational screen. We found that the reporter lines with the mutated S1 site (5′-TGTGAGAAT → 5′-Tcat-AGAAT) lack expression in both wing and haltere discs (Figure 5, B and E). When we mutated the S1 site in the context of the *nab-CDA* fragment (Figure 3A), we found diminished expression at the margin similar to the *nab-C* fragment (compare Figure 5D to Figure 4C). Thus, the Su(H) S1 site is absolutely necessary for *nab* DWME activity in both the cells along the dorsal margin and the anterior–posterior compartment cells located farther into the wing pouch.

The flanking Su(H) S2 site matches the consensus motif 5′-YGTGDGAAH, which is slightly less stringent than the genome screen motif 5′-YGTGRGAAH (Figure 3A). Nonetheless, this S2 site is still conserved across *Drosophila*. We found that reporter lines with the mutated S2 site (5′-CGTGTGAAA → 5′-CcatTGAAA) drive diminished expression that is collapsed to two small attenuated spots along the margin near the predicted peak pMad regions (Figure 5, C and E). Thus, the flanking S2 Su(H) site is also important for robust activation along the dorsal wing margin as well as in the off-margin spots.

To confirm that the Su(H) sites work canonically in Notch-dependent inducible activation, we also compared DWME activity from the *nab-A*-driven reporter in both wild-type and mutant Notch backgrounds (Figure 5, F–H). These experiments show that whereas wild-type Notch allows robust DWME activity in nearly 100% of wing imaginal discs, a Notch mutant background (N^1) results in ∼60% of the discs not having any expression at all and ∼40% of the discs having very weak expression close to the margin (Figure 5, F and H). Thus, the *nab* DWME requires both wild-type Notch signaling and both of its Su(H) binding sites for robust expression in the wing pouch. This signaling is also required for the off-margin expression in the anterior–posterior compartment "spots," suggesting that BMP input into the DWME is not independent of Notch signaling.

Su(H) binding sites are involved in interenhancer silencing

In the absence of NICD, Su(H) recruits Hairless and establishes a repression complex at many targeted enhancers (Bang *et al.* 1995; Barolo *et al.* 2002; Maier *et al.* 2011). Moreover, there is evidence for long-range looping of multiple Notch/Su(H)-targeted promoters from the *E(spl)* gene complex into an interaction domain associated with cohesin and the PRC1 polycomb repression complex (Schaaf *et al.* 2013). We thus hypothesize that some of the predicted Su(H) binding sites involved in Notch-dependent inducible activation might also be involved in interenhancer silencing or attenuation.

To test the hypothesis that the S1 Su(H) site within the DWME is responsible for silencing the ectopic larval brain activity associated with *nab-C*, we mutated this site in the *nab-CDA* fragment (Figure 3A). We find that mutation of this site does not result in ectopic expression in larval brains (data

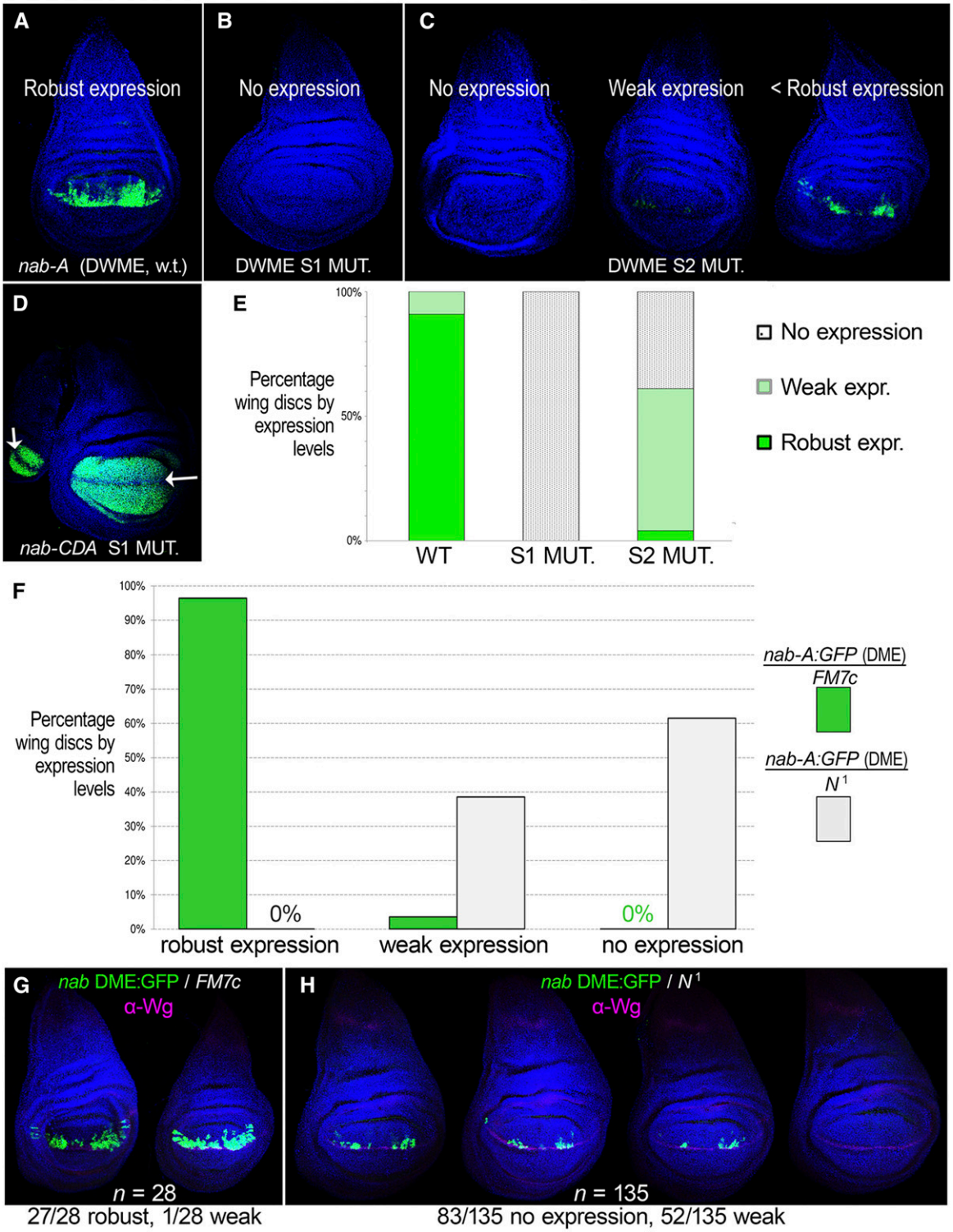

Figure 5 The *nab* DWME is induced by Notch signaling via its Su(H) sites. (A) The DWME contains two Su(H) sites, S1 and S2, and drives a unique stereotypical pattern. To test the role of these sites, we mutated each individually in the minimalized *nab-A* enhancer fragment. (B) The S1 mutated *nab-A* fragment exhibits no expression in wing imaginal discs. (C) The S2 mutated *nab-A* fragment results in discs with either no expression or weak dorsal margin expression as shown in these representative discs. (D) The *nab-CDA* fragment with an S1 mutated Su(H) exhibits reduced expression at the D–V compartment margin (arrow). (E) Quantitative comparison of wild-type, S1 mutated, and S2 mutated discs according to levels of expression. (F) Quantitative comparison of *nab-A* DWME activity in wild-type or mutant Notch backgrounds. Also shown is representative DWME reporter activity from discs in wild-type (G) or mutant Notch (H) backgrounds.

not shown). Nonetheless, it is still possible that the S2 site and/or additional lower-affinity sites, which we did not mutate, might participate singly or collectively in an intronic interenhancer repression complex featuring Su(H).

To test the hypothesis that the strong S3 Su(H) site present within the BrE is responsible for the silencing of the DWME, we mutated this site (5′-TGTGAGAAC → 5′-TcatAGAAC) in the *nab-AB* fragment (Figure 3). Normally, the DWME activity is completely silenced in the wild-type *nab-AB* fragment, and partially attenuated in the *nab-DAB* fragment. We find that mutation of this S3 Su(H) site in *nab-AB* rescues the twin spots of DWME activity in about half of the discs (16/30 discs), although at levels much diminished relative to the wild-type *nab-A* fragment (arrows in Figure 4I). Moreover, we also find that the hinge activity is much expanded along both the A–P axis and along the proximal–distal axis of the imaginal discs (Figure 4I). This suggests that the S3 Su(H) site is involved in both intraenhancer repression and interenhancer silencing/attenuation.

Apterous licenses the nab DWME to receive Notch/BMP signals in the dorsal wing compartment

We propose that selectors are not likely to act via recruitment of pQ-rich Mediator subunits as do the pQ-rich signaling effector activators. This is another reason to eschew the use of "activation" to describe the role of selectors and simply refer to their action as "licensing" (see *Discussion*). Motivated by a hypothesis of selector licensing of signal effector integration by enhancers, we used the binding motifs for the pQ-deficient selectors Ap, Sd, and Vg to identify the *nab* DWME as described above. In addition to the cluster of Ap binding sites, and the single Sd:Sd:Vg site, we also find a binding site for the homeotic selector Distalless (Dll) (5′-ATAATYAT), which has a similar expression pattern to Sd and Vg at the wing margin (Campbell and Tomlinson 1998). We thus suspect that the DWME might be licensed collectively by Sd, Vg, Dll, and Ap. Furthermore, like Ap, Sd, and Vg, Dll is also deficient in pQ and pN content.

While it will take future studies to show how multiple selectors might act collectively to regulate the *nab* DWME, we did seek to test the role of Ap, which has many candidate binding sites throughout the DWME. Expression of the selector Ap is restricted to the dorsal compartment of the wing pouch and the proximal parts of the wing imaginal disc (Cohen *et al.* 1992; Blair *et al.* 1994) (Figure 6A). In the absence of Ap, the DWME might be refractive to Notch and Dpp signaling, which are active in many contexts that do not feature *nab* DWME activity. To test the hypothesis that the *nab* DWME is licensed in part by Ap to respond to Notch and BMP developmental signals only in the dorsal wing compartment, we crossed our *nab* DWME reporter line into backgrounds differing in the dosage of normal Ap. As the levels of normal Ap is reduced, we observe that DWME-driven GFP reporter expression collapses to a smaller and smaller cluster of cells along the D–V border of each A–P compartment (Figure 6, B–D). This result is consistent with Ap being required for both robust expression along the margin and maintenance of DWME activity in off-margin descendants of margin cells.

Dorsal-compartment expression of nab is required for normal patterning of wing and thorax

Expression of *nab* in the dorsal compartment of the developing wing pouch is the result of cells using DWME and/or QE activity. To understand better the role of the DWME *vs.* the QE, we used the *ap-GAL4* hypomorph (ap^{GAL4}) to drive *nab* RNAi. This likely brings down *nab* mRNA levels in the dorsal compartment while also specifically disrupting the Ap-dependent activity of the endogenous *nab* DWME. Thus, in this experiment, the most severe disruption of *nab* expression is expected to be in the DWME-active cells.

Using one copy of the ap^{GAL4} allele to drive expression of UAS:*nab*-RNAi, we observe the following set of phenotypes. We observe an exaggerated creased wing along vein II (Figure 6E), which may be consistent with differences in Nab signaling between dorsal and ventral wing epithelia. This is often accompanied by a malformed delta-like junction between the first and second wing veins at the anterior margin (Figure 6E′). Sometimes this is accompanied by a disrupted bristle pattern at the juncture of the margin (Figure 6E′ *vs.* Figure 6F, wild type). In addition, the scutellum of these flies is malformed and diminished in size with typically one or more anterior and posterior scutellar bristles missing (compare Figure 6, G and H to Figure 6, I–K). In these flies, the anterior and posterior dorsocentrals in the notum are also frequently absent (Figure 6, I–K). Thus, there are missing or mis-specified macrochaetes in both the notum and scutellum. Wings from ap^{GAL4}:*nab*-RNAi adults show other defects including occasional ectopic wing veins, gaps in the wing vein patterning, and diminished or absent anterior cross-veins (data not shown). Therefore, we propose that normal patterns and/or levels of *nab* are required in the dorsal margin cells to ensure proper wing vein specification and patterning.

The results of dorsal compartment-specific knockdown of *nab* suggests that expression levels are critical to morphogenetic pattering of the notum and wing veins (Figure 6). To explore further the importance of *nab* expression in wing imaginal discs, we expressed *nab*-RNAi in two additional ways. First, we used an endogenous *GAL4-nab* enhancer trap line (nab-NP3537) to drive the same *nab*-RNAi transgene. The prediction is that in this experiment, both endogenous Nab and Gal4 proteins are being synthesized simultaneously as the result of the different regulatory enhancers at *nab* inducing transcription of both *nab* and *GAL4*. Thus, this experiment might be expected to result in only a partial knockdown of Nab protein because of the delayed transcriptional/translational cycle of Gal4-driven *nab*-RNAi. In this experiment, we observe the mildest effect of all the *nab*-RNAi experiments in that we only observed one phenotype: occasional loss of the posterior cross-veins but only in adult females (see arrows in Figure 7, B and C).

To test the role of *nab* expression in other wing disc compartments, we used an *engrailed* (*en*) *GAL4* enhancer trap line

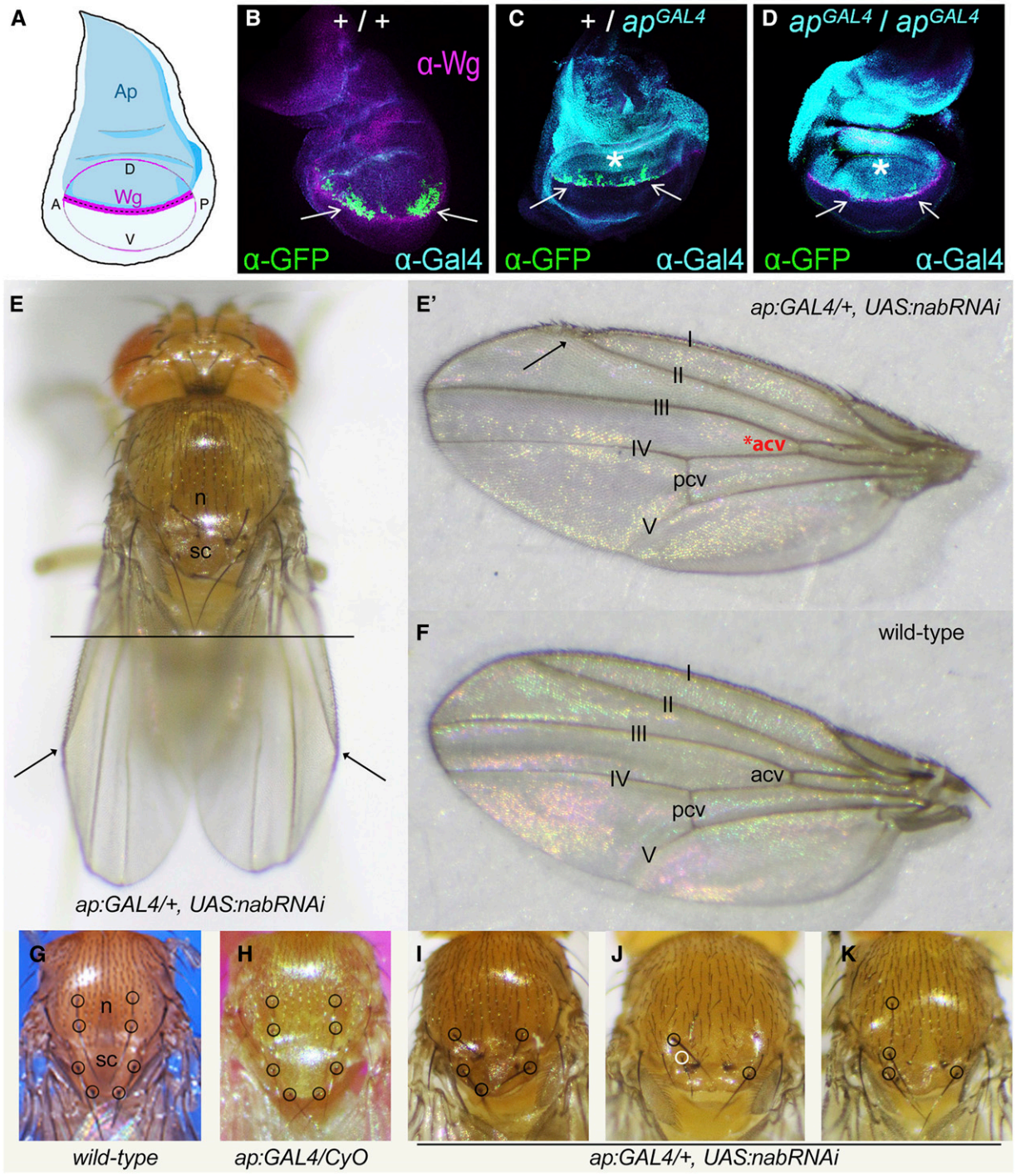

Figure 6 Apterous licenses the *nab* DWME to be receptive to Notch and Dpp signaling in the dorsal compartments of wing imaginal discs. (A) Cartoon of Ap expression (blue) in the dorsal compartment of a third instar wing imaginal disc. Wingless (Wg) expression (magenta) is found at the D–V compartment boundary in the wing pouch. (B–D) Wing imaginal discs stained for Wg (magenta), Gal4 (cyan), and GFP (green) in a line carrying the *nab-A* (DWME) eGFP reporter in a wild-type Ap background (B), in a heterozygous *ap-GAL4* hypomorph caused by a *GAL4* element integration (C), and a homozygous *ap-GAL4* hypomorph (D). Note as the intensity of the Gal4 signal increases, the *nab* DWME-driven GFP signal decreases, which is consistent with its many Ap binding sites. (E and E′) The same *ap-GAL4* hypomorph was used to drive *nab* RNAi to knock down expression in the dorsal compartment via both RNA and enhancer interference. Defects include an overly creased wing at wing vein II (arrows in E), a delta-like patterning defect where wing veins I and II intersect (arrow in E′), and occasionally missing or diminished anterior cross-veins (*acv). (F) Wild-type wing for comparison to E. (G) Wild-type notum (n) and scutellum (sc) with macrochaetes circled. (H) One balanced copy of the *ap-GAL4* does not affect macrochaete patterning nor development of the scuttelum. (I–K) When *ap-GAL4* drives *nab*-RNAi, adult flies develop grossly misshapen scutellums with severe macrochaete patterning defects. Three representative thoraxes are shown.

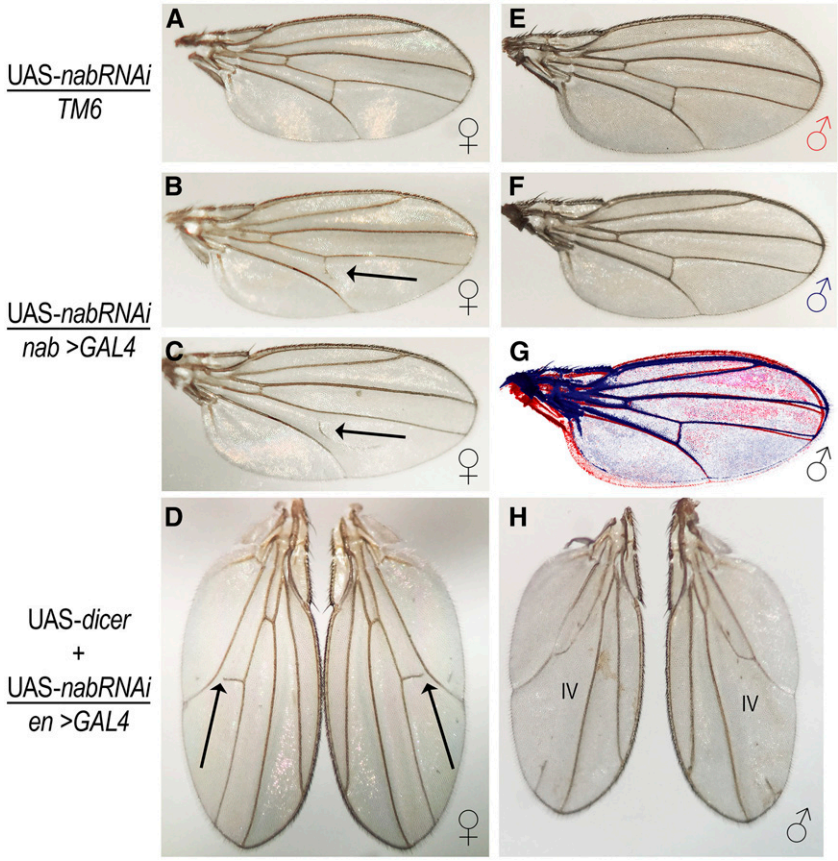

Figure 7 Distinct levels of nab expression are required for normal developmental patterning of the notum, scutellum, and wing veins. Wing vein patterning in female (A–D) and male (E–H) fly wings carrying a UAS-*nab*-RNAi transgene without a GAL4 driver (A, E, and the red wing outline in G), a *nab* locus GAL4 enhancer trap driver (B, C, F, and blue wing outline in G), or an *en* locus GAL4 enhancer trap driver augmented with additional UAS-*dicer* expression (D and H). Posterior cross-veins are often lost or incomplete in female wings with *nab*-RNAi knockdown arrows (B–D). The fourth wing vein is often lost in male wings (H). Thus, normal patterns of *nab* expression in both the dorsal and ventral compartments are crucial to wing vein patterning.

to drive *nab*-RNAi in the posterior compartment, which spans both D–V compartments (see *Material and Methods*). En is a selector protein expressed early in the posterior compartments of wing imaginal discs, where it determines posterior-compartment identity (growth/size, shape, and wing vein patterning) (Lawrence and Morata 1976; Kornberg 1981; Blair 1992; Brower 1986). Importantly, in the *en-GAL4* experiment, *nab*-RNAi would be induced and maintained prior to transcription of *nab* in early third instar wing imaginal discs (Terriente Félix *et al.* 2007). To increase the severity of any phenotypes, we used the *en-GAL4* transgene to drive both *UAS-nab*-RNAi and *UAS-dicer*. This experiment results in a more severe wing vein patterning defect in both females and males (Figure 7, D and H, respectively). This phenotype, which includes incomplete and missing longitudinal veins as well as cross-veins, is restricted to the posterior compartment. We do not see any morphological defects in scutellar development, suggesting that *ap* hypomorphs sensitize scutellar development to loss of Nab function.

In summary, *nab*-RNAi knockdown experiments demonstrate that *nab* expression is important in all compartments of wing imaginal discs, including both proximal and distal parts of discs, for the normal developmental patterning of the scutellum, thoracic macrochaetes, and wing veins. This is consistent with *nab*'s intronic complex of three wing imaginal disc enhancers (QE, PWE, and DWME).

The nab DWME is a lineage-specific enhancer maintaining expression in off-margin clonal descendants of margin cells

To better understand the individual roles of the *nab-A* binding sites mediating Notch and Dpp signaling, we examined the developmental onset of expression in wing imaginal discs. We find that DWME-driven expression begins around late second/early third instar discs in a few cells at the margin (Figure 8, A and B). This is consistent with the earliest reported detection of Nab protein in early third instar discs (Terriente Félix *et al.* 2007). As the discs develop, there are many examples of dividing daughter cells in which one of the daughter cells is dividing away from the D–V boundary while still maintaining equivalent amounts of expression (see circled pairs of cells in Figure 8, A′–D′ and I′). This is not simply due to stable GFP inheritance in margin daughter cells because these dividing pairs of cells can also be seen at much farther distances from the margin in later stages (Figure 8I′). We also observe decreasing DWME-driven reporter activity in early-to-mid third instar cells along the margin when peak pMad is still centralized as a single (*i.e.*, nonbimodal) peak (see series of arrows of decreasing size in Figure 8I′).

This temporal profile of *nab* DWME activity suggested to us that the DWME marks a clonal patch of cells descended from a margin cell, which experienced early Notch–Delta signaling (see Figure 9B and *Discussion*). This would also explain a role for the Dpp input in stabilizing activity of the

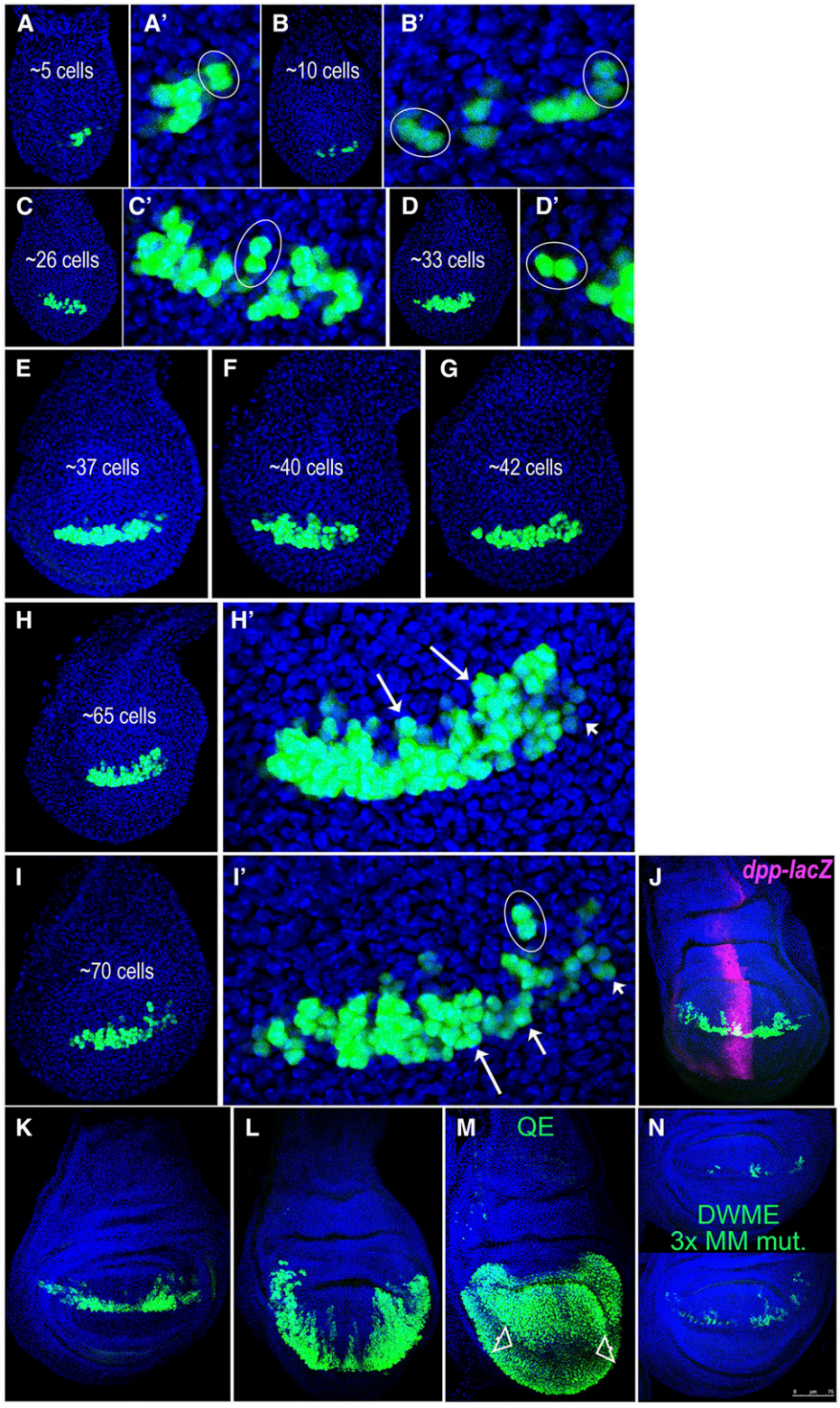

Figure 8 The *nab* DWME is stably maintained in off-margin clonal descendants. (A–L) GFP reporter activity driven by the *nab* DWME (*nab-A* fragment) starting during late second instar to late third instar wing imaginal discs are shown arranged according to the number of expressing cells based on nuclear GFP intensity. (A′–D′, H′, and I′) Zoomed-in images. Inspection of recently divided daughter cells (*e.g.*, ovals in A′–D′ and I′) demonstrate that GFP activity is equally maintained in both cells even when the direction of cytokinesis places one of the daughter cells farther away from the dorsal compartment boundary. Cells far removed from the D–V boundary but still near the A–P compartment boundary display robust GFP expression (large arrows in H′). However, cells farther away from the A–P compartment boundary display decreasing levels of GFP expression even when they are on the dorsal margin itself (smaller arrows in H′ and I′). During early–late third instar (J and K) and late–late third instar/prepupal (L) discs, the DWME activity is maintained in clonal descendants of dorsal margin cells that are now located deep into the wing pouch. We thus propose that the DWME functions as a lineage-specific margin enhancer that maintains expression in dorsal off-margin clonal descendants. The disc in J is doubled stained for β-gal (magenta) driven by a 3-kb *dpp* enhancer (see *Material and Methods*). (M) The *nab* QE (*nab-B* fragment) is noticeably weaker or not active in dorsal compartment off-margin cells (arrowheads) from late third instar/prepupal discs. (N) DWME fragment in which all three Mad:Medea binding sequences have been mutated (5′-CG to 5′-TT mutations at each site) drives diminished expression in both margin and off-margin cells. Two representative discs are shown.

DWME in clonal descendants removed from the border of active Notch–Delta signaling. Like clonal fate mapping in wing imaginal discs (Dahmann and Basler 1999), cells expressing DWME-driven GFP are patch-like clusters of dividing cells that respect both D–V and A–P compartment boundaries. Consistent with this idea, DWME-driven patches of GFP expression resemble the D–V-oriented cell proliferation patterns made by marked clones in wing imaginal discs (González-Gaitán *et al.* 1994). To explore this idea further, we also looked at the *nab* QE (*nab-C*) reporter in late third

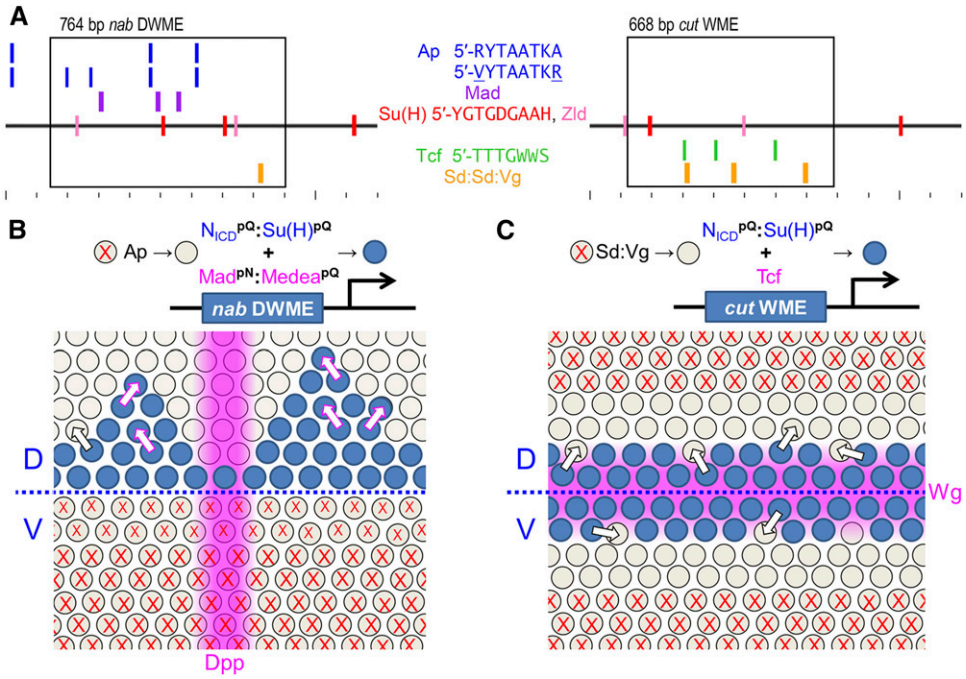

Figure 9 An enhancer model featuring selector licensing for pQ-mediated signal integration. (A) Shown are the trascription factor binding site motif distributions for the *nab* DWME (left) and the *cut* WME (right), both of which are induced by Notch signaling and Su(H) binding sites. As much as possible, matches to the indicated motifs are shown on separate tracks for ease of visualization. Tick marks represent 100-bp intervals. Boxes represent the minimalized enhancers, but in both cases, augmented expression is seen with larger fragments. (B and C) Below each enhancer are models of how each enhancer works in the context of both homeotic licensing and graded pQ signal integration or lack thereof. In both examples, selectors are envisioned as allowing certain cells (cell without Xs) to be receptive to transcriptional effectors of signaling pathways (Notch, Dpp, and Wg). The pQ/pN-rich Mad:Medea complexes are envisioned as stabilizing the active DWME in daughter cells of margin cells (B). In contrast, no such stabilizing effect is envisioned for the *cut* WME, which lacks both Mad:Medea sites (purple boxes) and instead has only Tcf (green boxes) and Su(H) (red boxes) binding sites (C). Thus, this enhancer would become inactive in margin daughter cells that divide away from the margin border, where there is active Notch–Delta signaling.

instar/prepupal wing imaginal discs specifically to see if the deficiency in dorsal margin expression becomes more noticeable over time. We find that this is possibly the case as the margin gap appears more pronounced than earlier stages (compare arrowheads in Figure 8M to Figure 4C or Figure 4C′′′).

The DWME temporal profile suggests that the *nab* DWME and QE are complementary lineage-specific enhancers that have evolved to deliver Nab expression in proliferating wing pouch cells more uniformly than what the QE alone could drive. To test the hypothesis that the identified Mad:Medea binding sequences in the DWME are critical for maintaining expression in the margin gap evident in QE reporter activity in late third instar, we mutated all three Mad:Medea sites in the *nab-A* (DWME) fragment by changing the motif-prominent 5′-CG dinucleotide in each binding sequence to 5′-TT (see Figure S1). We find that these mutations result in substantially weakened expression in both the margin cells and in the off-margin descendants of margin cells (Figure 8N). This suggests that the Dpp/BMP signaling input is required for both synergistic activation with Notch signaling at the margin and for stabilization of DWME activity in off-margin descendants. Furthermore, it also suggests that the DWME functions to rescue a QE "signaling hole."

Discussion

We used a comparative genomics approach to identify and characterize a novel enhancer mediating tissue-compartment specific activation based on the integration of two signaling pathways: Notch and BMP/Dpp. This approach led us to a dense intronic cluster of binding sites for the desired activators and selectors at the *Drosophila* gene *nab*. "Nab" was named for "NGFI-A binding" and is present in vertebrates as Nab1 and Nab2, where they work as corepressors of the C_2H_2 zinc finger factors Egr1 (NGFI-A/Krox24) and Egr2 (Krox20) to control proliferation, patterning, and differentiation (Russo *et al.* 1995; Svaren *et al.* 1996). Similarly in the nematode *Caenorhabditis elegans*, this gene encodes MAB-10/NAB, which is a corepressor of the LIN-29/EGR C_2H_2 zinc finger factor and is involved in cellular differentiation (Harris and Horvitz 2011). In *Drosophila*, LIN-29 functions appear to be maintained across three paralogous genes encoding C_2H_2 zinc finger factors: *rotund* (*rn*), *squeeze*, and *lin19* (Vilella *et al.* 2009). Correspondingly, *Drosophila* Nab functions as a corepressor of Rn in wing imaginal discs and as a coactivator of Squeeze in a subset of embryonic neuroblasts (Terriente Félix *et al.* 2007), but a Nab cofactor function for the putative fly Egr1/2 ortholog encoded by the *stripe* gene has yet to be identified. Nonetheless, *nab* is conserved across bilaterian animals and encodes a cofactor of specific C_2H_2 zinc finger transcription factors involved in developmental patterning and differentiation.

The dense site cluster that we identified in the first intron of *nab* drives a novel expression pattern that is consistent with integration of a D–V Notch signal and an orthogonal A–P BMP signal. The *nab* locus is already known to be induced by Dpp/BMP signaling (Ziv *et al.* 2009; Hadar *et al.* 2012). This is consistent with our finding several canonical Mad:Medea binding sequences in the *nab* DWME (Figure 3A) and several

low-affinity Mad:Medea binding sequences in the *nab* QE (not shown). Furthermore, both the DWME and QE drive A–P-modulated expression in the wing pouch (Figure 4, B, C, B′′′, and C′′′). We find that the *nab* DWME has at least two canonical Su(H) binding sites that are critical to its activity at the D–V margin. This activity is also impacted by a mutant *Notch* background. Similarly, we find that one to three SMAD binding sites are essential for the Notch/BMP signal integration. Thus, this may be the first example of a wing disc enhancer that is downstream of both Notch and BMP signaling. By virtue of its obligate Notch signaling input, the DWME's transcriptional readout of the BMP morphogen gradient is an idealized two-dimensional graph of pMad levels (*y*-axis) at different A–P positions (*x*-axis).

To deconstruct the developmental role of *nab* expression in different wing compartments, we used the *ap-GAL4* enhancer trap to drive *nab*-RNAi in the dorsal compartment. This RNAi experiment would also knockdown activity of the Ap-dependent dorsal wing margin enhancer in the dorsal wing compartment. With this manipulation, we observed morphogenetic defects of both the thorax and the wing, suggesting an important role for Nab in developmental patterning of the dorsal compartment. More specifically, the patterning defects affect the scutellum and thoracic macrochaetes, consistent with both *nab* expression and its PWE. This experiment also resulted in an increased rate of wing vein patterning defects. We also observed similar wing vein patterning defects, including loss of the posterior cross-vein in males and females and loss of longitudinal veins IV and V in males, when we drove *UAS:nab*-RNAi in the posterior compartment using an *en-GAL4* enhancer trap line. A milder knockdown using a *nab-GAL4* enhancer trap line resulted in an increased loss of the posterior cross-vein in adult females. Thus, of all the knockdown phenotypes, developmental specification of the posterior cross-vein was the most sensitive to diminished Nab function. This is an interesting finding given that *crossveinless c* was the only other locus in the genome having a similar cluster of binding sites as the *nab* DWME (Table 1).

Lineage-specific aspects of wing margin and wing quadrant enhancers

Inspection of the site composition of the *nab* DWME shows it is similar to the WME at *cut* (Figure 9A). Both wing margin enhancers are induced by Notch signaling and have functional sites for Su(H) (Jack *et al.* 1991; Neumann and Cohen 1996a). We find both enhancers also have sequences matching the binding preferences for Zelda and Scalloped:Scalloped dimers, although the *cut* WME has many more of the latter. However, the *nab* and *cut* wing margin enhancers each have multiple binding sites either for Mad:Medea or for Tcf, but not for both (compare purple SMAD sites in the *nab* DWME *vs.* green Tcf sites in the *cut* WME in Figure 9A). Unlike the Mad:Medea complex, *Drosophila* Tcf/Pangolin and its β-catenin coactivator Armadillo, which together mediate Wg/WNT signaling, are not pQ/pN-rich. We thus propose the following model for pQ-mediated Notch/BMP signal integration at the *nab* DWME (Figure 9B) that distinguishes it from the *cut* WME (Figure 9C).

We hypothesize that pQ/pN-mediated aggregation of Mad:Medea and Su(H):NICD complexes produced by the *nab* DWME stabilizes and maintains an active DWME in off-margin clonal descendants of D–V margin cells. Thus, the *nab* DWME would remain active only in daughter cells that are also simultaneously experiencing high levels of nuclear pMad (see arrows in Figure 9B). In contrast, the *cut* WME would become inactive in these same off-margin daughter cells because they are no longer experiencing Notch or Wg signaling (see arrows in Figure 9C). In this way, the *nab* DWME functions as a lineage-specific enhancer in regions with active phosphorylated-Mad (pMad). In contrast, the *cut* WME is not lineage-specific because its activity is extinguished in cell descendants as they divide away from the margin. Consistent with this model of Notch/BMP integration at the *nab* DWME, the presumed pMad input is not sufficient for driving DWME expression in cells that although having peak pMad levels are not descended from margin cells.

The *cut* locus is not expressed throughout the wing pouch like the *nab* and *vg* genes, both of which have separate margin/boundary and quadrant enhancers. This also highlights the lineage specificity of some wing pouch enhancers as follows. The *vg* locus contains a Notch-target boundary enhancer (Williams *et al.* 1994) as well as a separate BMP-target quadrant enhancer (Kim *et al.* 1997). The *vg* boundary enhancer drives expression broadly throughout the presumptive wing border region while the *nab* DWME drives expression in dorsal margin cells and their off-margin descendants. While the *vg* locus has separate "single-channel" enhancers responsive to either Notch or BMP signaling pathways, the *nab* locus has enhancers responsive to combined Notch/BMP signals and (presumably) BMP-only signals. Nonetheless, separate margin/boundary and quadrant enhancers would be required by loci expressed uniformly in proliferating cells of the developing wing pouch. Potentially, this "rule" might generalize across diverse developmental systems in which a gene is expressed broadly in a proliferating tissue patterned by a smaller number of compartment organizer cells. One enhancer would respond to signals experienced specifically by organizer cells, and a second enhancer would respond to signals experienced more broadly across the developmental field.

Our study of the *nab* intronic enhancer complex also demonstrates a remarkable aspect of transcriptional enhancers. We found that all of the *nab* intronic enhancers are also silencers. This is reminiscent of studies in *Drosophila* and mammals identifying arrays of dual enhancer–silencer modules acting in concert to drive complex patterns of gene expression (Sasaki and Hogan 1996; Bessis *et al.* 1997; Holohan *et al.* 2006; Perry *et al.* 2011). Examples of mutual enhancer inhibition also have been found to involve insulators and core promoters (Lin *et al.* 2007).

Importantly, we discovered the many *nab* dual enhancer–silencer activities because we were monitoring expression

across several tissues of the embryo, larva, and pupa. These results and others suggest that we should be cautious about the effects of enhancer ("over")-minimalization. The "cryptic" silencer aspect of enhancers may predispose tissue-specific enhancer screens to high false-positive rates of detection if short regulatory DNA fragments are associated with ectopic activities. In any case, these results suggest a new role for Su(H) in mediating interenhancer silencing and attenuation. This functional role is worth testing in greater depth across several additional examples.

Selectors: licensing factors via nucleosomal positioning?

Homeotic selectors were defined initially as TFs that decide and maintain a choice of alternate cell fate potentials for a clonal population of cells and their descendants (García-Bellido 1975; Lawrence *et al.* 1979). One early clue suggesting that they correspond to a specific regulatory mechanism was that (homeotic) selectors in animals were predominantly found in the form of homeodomain-containing factors (McGinnis *et al.* 1984). While selectors were initially discussed in terms of cell fate determination and cell fate potential, a consideration of evolutionary processes suggested an emphasis on the role of transcriptional enhancers as important components of selector-based regulation (Akam 1998). Thus, we hypothesize that the phenomenology of selectors acting on cell fate decisions lies in their roles as factors licensing enhancer DNAs to receive graded developmental signals through any number of pathways (*e.g.*, Notch, BMP/Dpp, WNT/Wg, and Hh). For reasons explained below, we further hypothesize that selectors could work simply through nucleosome repositioning, while signal pathway effectors could work through pQ-mediated aggregation and Mediator recruitment.

We have referred to selector activity as licensing and the pathway effector activity as (true) activation for two additional reasons. First, licensing via the fixation of alternate fixed nucleosomal positions could function phenomenologically both in transcriptional activation and in repression, depending on whether effector sites are being revealed or occluded with the positional shifting of a fixed nucleosome. Second, signaling pathway-based effectors tend to be pQ-rich like the Mediator coactivator complex (Tóth-Petróczy *et al.* 2008) and TBP (Koide *et al.* 1999), which are recruited by pathway-effector TFs. Thus, signaling pathway integration via pQ-mediated aggregation would be inherent to eukaryotic activation. It would also be functionally rich because it reserves an important role for *cis*-element organization to strengthen an otherwise nonspecific protein–protein interaction.

The *nab* DWME, *nab* QE, *cut* WME, and *vg* WME (*i.e.*, the boundary enhancer, BE) have binding sites for homeotic selectors in addition to those for the pathway-mediating effectors. Selectors can act in a negative or positive manner as demonstrated by known wing disc enhancers. The *vg* WME uniquely has matching sites for the posterior Hox factor Abd-B homeotic selector (5′-YYTTTATGK) that are not found in either the *nab* or *cut* WMEs (data not shown). Abd-B plays a negative selector role by prohibiting expression of *vg* in posterior segments (Carroll *et al.* 1995). Similarly, the *nab* QE possesses binding sites for Homothorax (Hth) (5′-ARYDATSRC), which is known to ChIP to this enhancer (Slattery *et al.* 2013). Hth is expressed throughout the disc except in the wing pouch and is thus likely to prohibit expression outside of the wing pouch. This would be consistent with the clean border of *nab* QE reporter expression at the wing pouch/hinge border. In contrast, Hth sites are absent in the *vg* WME, which drives D–V margin expression beyond the pouch.

The wing margin enhancers at *nab* and *cut* are likely to use positively acting selectors. Consistent with the site composition of the *nab* and *cut* WMEs (Figure 9A), the former would be positively licensed primarily by the selector Ap for the dorsal wing compartment (see cells without Xs in Figure 9B), while the latter would be positively licensed by the selector complex of Sd and Vg (see cells without Xs in Figure 9C). Thus, a mutant Ap background causes DWME-driven expression to collapse to a few cells along the wing margin. Because of the dorsal compartment-specific expression of Ap, and the known localization of activity of Notch signaling to the margin, it is the Notch pathway, secondarily augmented by the BMP input, that drives its expression pattern. Ap only marks a larger domain in which DWME activity can occur. Thus, we interpret this as Ap "licensing" the Notch-dependent DWME for expression exclusively in the dorsal compartment. Additional positively acting selectors are likely to work at the *nab* DWME based on conservation of known binding sequences, but further work will be required to elucidate these more definitively.

Certain sequence features in the *nab* DWME hint at the role of selectors in making the enhancer sequences either receptive or refractory to effector DNA binding via fixed or remodeled nucleosomal positions. The core sequence of the DWME overlaps fixed nucleosomal positions in early embryonic stages prior to DWME activity (Figure S4) (Mavrich *et al.* 2008; Langley *et al.* 2012). At specific sites flanking these fixed nucleosomes, there are also polyT, homopolymeric runs (Figure S4), which can act as nucleosome repulsing sequences (Anderson and Widom 2001; Segal and Widom 2009). In addition, we also see evidence for competing TT/AA/TA dinucleotide phasing embedded at these fixed nucleosomal windows (Lowary and Widom 1998; Thåström *et al.* 1999; Segal *et al.* 2006). Based on the known Su(H) binding structures (Arnett *et al.* 2010), these fixed positions would make the central S1 Su(H) site unavailable for binding (Figure S4). We thus suggest that some selectors may act by binding and stabilizing alternate nucleosomal positions that reveal effector binding sites. Intriguingly, we also find that Apterous binding sites coincide with the nucleosomal DNA entry regions that are also associated with the repressor linker histone H1 (Syed *et al.* 2010). Consistent with the inability of Su(H) to bind the DWME sites in the absence of Ap, we find that Su(H) ChIP signals at the *nab* DWME have not been detected in embryonic stages (Nègre *et al.* 2011).

We thus speculate that the above homeodomain-containing selectors (Ap, Dll, Hth) and other selectors (*e.g.*, Sd and Vg) work via a mechanism that is different from the graded spatial (Notch/BMP) and temporal (Zld) patterning effectors. The above set of selectors are deficient in pQ (Figure 1A), pN (Figure 1B), and mixed p(Q/N) carboxamide (Figure 1C) tracts unlike the spatiotemporal effectors and the Mediator coactivator complex, which they recruit in their role as activators. We suggest that the phenomenon of graded signal integration by effectors also occurs via generic polycarboxamide aggregation as dictated by the composition of binding sites present in different DNA enhancer scaffolds. In stark contrast, pQ/pN-deficient selectors could bind and fix (*i.e.*, stabilize) default or alternate nucleosomal positions without cross-interacting with pQ/pN-rich effectors. Furthermore, the relationship between selector and pathway effector binding sites would be informed by a helically phased "regulatory reading frame" based on nucleosomal positioning.

Acknowledgments

We thank Timothy Fuqua for assistance with some of the antibody staining protocols and Bryan Phillips and Timothy Fuqua for comments on early versions of this manuscript. This work was supported in part by a National Science Foundation CAREER award to A.E. to study morphogen gradient enhancer readouts (IOS:1239673), National Institutes of Health T-32 bioinformatics training grant support to E.S., and two Evelyn Hart Watson research fellowships (in 2014 and 2015) to E.S.

Literature Cited

Akam, M., 1998 Hox genes, homeosis and the evolution of segment identity: no need for hopeless monsters. Int. J. Dev. Biol. 42: 445–451.

Anderson, J. D., and J. Widom, 2001 Poly(dA-dT) promoter elements increase the equilibrium accessibility of nucleosomal DNA target sites. Mol. Cell. Biol. 21: 3830–3839.

Archbold, H. C., C. Broussard, M. V. Chang, and K. M. Cadigan, 2014 Bipartite recognition of DNA by TCF/Pangolin is remarkably flexible and contributes to transcriptional responsiveness and tissue specificity of wingless signaling. PLoS Genet. 10: e1004591.

Arnett, K. L., M. Hass, D. G. McArthur, M. X. G. Ilagan, J. C. Aster *et al.*, 2010 Structural and mechanistic insights into cooperative assembly of dimeric Notch transcription complexes. Nat. Struct. Mol. Biol. 17: 1312–1317.

Artavanis-Tsakonas, S., 1999 Notch signaling: cell fate control and signal integration in development. Science 284: 770–776.

Bang, G., M. Bailey, and J. W. Posakony, 1995 Hairless promotes stable commitment to the sensory organ precursor cell fate by negatively regulating the activity of the Notch signaling pathway. Dev. Biol. 172: 479–494.

Barad, O., E. Hornstein, and N. Barkai, 2011 Robust selection of sensory organ precursors by the Notch-Delta pathway. Curr. Opin. Cell Biol. 23: 663–667.

Barolo, S., T. Stone, A. G. Bang, and J. W. Posakony, 2002 Default repression and Notch signaling: hairless acts as an adaptor to recruit the corepressors Groucho and dCtBP to suppressor of hairless. Genes Dev. 16: 1964–1976.

Barolo, S., B. Castro, and J. W. Posakony, 2004 New *Drosophila* transgenic reporters: insulated P-element vectors expressing fast-maturing RFP. Biotechniques 36: 436–442.

Bergman, C. M., J. W. Carlson, and S. E. Celniker, 2005 *Drosophila* DNase I footprint database: a systematic genome annotation of transcription factor binding sites in the fruitfly, *Drosophila melanogaster*. Bioinformatics 21: 1747–1749.

Bessis, A., N. Champtiaux, L. Chatelin, and J. P. Changeux, 1997 The neuron-restrictive silencer element: a dual enhancer/silencer crucial for patterned expression of a nicotinic receptor gene in the brain. Proc. Natl. Acad. Sci. USA 94: 5906–5911.

Bhaskar, V., M. Smith, and A. J. Courey, 2002 Conjugation of Smt3 to dorsal may potentiate the *Drosophila* immune response. Mol. Cell. Biol. 22: 492–504.

Blair, S. S., 1992 *engrailed* expression in the anterior lineage compartment of the developing wing blade of *Drosophila*. Development 115: 21–33.

Blair, S. S., D. L. Brower, J. B. Thomas, and M. Zavortink, 1994 The role of apterous in the control of dorsoventral compartmentalization and PS integrin gene expression in the developing wing of Drosophila. Development 120: 1805–1815.

Bray, S., and M. Furriols, 2001 Notch pathway: making sense of Suppressor of Hairless. Curr. Biol. 11: R217–R221.

Brittain, A., E. Stroebele, and A. Erives, 2014 Microsatellite repeat instability fuels evolution of embryonic enhancers in Hawaiian *Drosophila*. PLoS One 9: e101177.

Brower, D. L., 1986 Engrailed gene expression in Drosophila imaginal discs. EMBO J. 5: 2649–2656.

Campbell, G., and A Tomlinson, 1998 The roles of the homeobox genes aristaless and Distal-less in patterning the legs and wings of Drosophila. Development 125: 4483–4493.

Campbell, G., and A. Tomlinson, 1999 Transducing the Dpp morphogen gradient in the wing of *Drosophila*. Cell 96: 553–562.

Carroll, S. B., S. D. Weatherbee, and J. A. Langeland, 1995 Homeotic genes and the regulation and evolution of insect wing number. Nature 375: 58–61.

Clements, M., D. Duncan, and J. Milbrandt, 2003 *Drosophila* NAB (dNAB) is an orphan transcriptional co-repressor required for correct CNS and eye development. Dev. Dyn. 226: 67–81.

Cohen, B., M. E. McGuffin, C. Pfeifle, D. Segal, and S. M. Cohen, 1992 apterous, a gene required for imaginal disc development in Drosophila encodes a member of the LIM family of developmental regulatory proteins. Genes Dev. 6: 715–729.

Courey, A. J., and R. Tjian, 1988 Analysis of Sp1 in vivo reveals multiple transcriptional domains, including a novel glutamine-rich activation motif. Cell 55: 887–898.

Courey, A. J., D. A. Holtzman, S. P. Jackson, and R. Tjian, 1989 Synergistic activation by the glutamine-rich domains of human transcription factor Sp1. Cell 59: 827–836.

Cowden, J., and M. Levine, 2002 The Snail repressor positions Notch signaling in the *Drosophila* embryo. Development 129: 1785–1793.

Crocker, J., and A. Erives, 2013 A Schnurri/Mad/Medea complex attenuates the dorsal-twist gradient readout at vnd. Dev. Biol. 378: 64–72.

Crocker, J., Y. Tamori, and A. Erives, 2008 Evolution acts on enhancer organization to fine-tune gradient threshold readouts. PLoS Biol. 6: 2576–2587.

Crocker, J., N. Potter, and A. Erives, 2010 Dynamic evolution of precise regulatory encodings creates the clustered site signature of enhancers. Nat. Commun. 1: 99.

Dahmann, C., and K. Basler, 1999 Compartment boundaries: at the edge of development. Trends Genet. 15: 320–326.

de Celis, J. F., 1997 Expression and function of decapentaplegic and thick veins during the differentiation of the veins in the Drosophila wing. Development 124: 1007–1018.
Erives, A., and M. Levine, 2004 Coordinate enhancers share common organizational features in the *Drosophila* genome. Proc. Natl. Acad. Sci. USA 101: 3851–3856.
Fortini, M. E., and S. Artavanis-Tsakonas, 1994 The suppressor of hairless protein participates in notch receptor signaling. Cell 79: 273–282.
Furukawa, T., Y. Kobayakawa, K. Tamura, K. Kimura, and M. Kawaichi *et al*., 1995 Suppressor of hairless, the *Drosophila* homologue of RBP-J kappa, transactivates the neurogenic gene *E(spl)m8*. Jpn. J. Genet. 70: 505–524.
García-Bellido, A., 1975 Genetic control of wing disc development in Drosophila. Ciba Found. Symp. 0: 161–182.
Gerlitz, O., D. Nellen, M. Ottiger, and K. Basler, 2002 A screen for genes expressed in *Drosophila* imaginal discs. Int. J. Dev. Biol. 46: 173–176.
González-Gaitán, M., M. P. Capdevila, and A. García-Bellido, 1994 Cell proliferation patterns in the wing imaginal disc of *Drosophila*. Mech. Dev. 46: 183–200.
Guruharsha, K. G., M. W. Kankel, and S. Artavanis-Tsakonas, 2012 The Notch signalling system: recent insights into the complexity of a conserved pathway. Nat. Rev. Genet. 13: 654–666.
Hadar, N., S. Yaron, Z. Oren, O. Elly, W. Itamar *et al.*, 2012 A screen identifying genes responsive to Dpp and Wg signaling in the *Drosophila* developing wing. Gene 494: 65–72.
Halder, G., and S. B. Carroll, 2001 Binding of the Vestigial cofactor switches the DNA-target selectivity of the Scalloped selector protein. Development 128: 3295–3305.
Halder, G., P. Polaczyk, M. E. Kraus, A. Hudson, J. Kim *et al.*, 1998 The Vestigial and Scalloped proteins act together to directly regulate wing-specific gene expression in *Drosophila*. Genes Dev. 12: 3900–3909.
Harris, D. T., and H. R. Horvitz, 2011 MAB-10/NAB acts with LIN-29/EGR to regulate terminal differentiation and the transition from larva to adult in *C. elegans*. Development 138: 4051–4062.
Harrison, M. M., X.-Y. Li, T. Kaplan, M. R. Botchan, and M. B. Eisen, 2011 Zelda binding in the early *Drosophila melanogaster* embryo marks regions subsequently activated at the maternal-to-zygotic transition. PLoS Genet. 7: e1002266.
Hayashi, S., K. Ito, Y. Sado, M. Taniguchi, A. Akimoto *et al.*, 2002 GETDB, a database compiling expression patterns and molecular locations of a collection of gal4 enhancer traps. Genesis 34: 58–61.
Helms, W., H. Lee, M. Ammerman, L. Parks, M. A. Muskavitch *et al.*, 1999 Engineered truncations in the *Drosophila mastermind* protein disrupt Notch pathway function. Dev. Biol. 215: 358–374.
Holohan, E. E., P. I. zur Lage, and A. P. Jarman, 2006 Multiple enhancers contribute to spatial but not temporal complexity in the expression of the proneural gene, *amos*. BMC Dev. Biol. 6: 53.
Housden, B. E., A. Terriente-Felix, and S. J. Bray, 2014 Context-dependent enhancer selection confers alternate modes of notch regulation on *argos*. Mol. Cell. Biol. 34: 664–672.
Hudson, J. B., S. D. Podos, K. Keith, S. L. Simpson, and E. L. Ferguson, 1998 The *Drosophila Medea* gene is required downstream of *dpp* and encodes a functional homolog of human Smad4. Development 125: 1407–1420.
Jack, J., D. Dorsett, Y. Delotto, and S. Liu, 1991 Expression of the cut locus in the Drosophila wing margin is required for cell type specification and is regulated by a distant enhancer. Development 113: 735–747.
Janody, F., and J. E. Treisman, 2011 Requirements for mediator complex subunits distinguish three classes of notch target genes at the *Drosophila* wing margin. Dev. Dyn. 240: 2051–2059.
Kelly, D. F., R. J. Lake, T. Walz, and S. Artavanis-Tsakonas, 2007 Conformational variability of the intracellular domain of *Drosophila* Notch and its interaction with Suppressor of Hairless. Proc. Natl. Acad. Sci. USA 104: 9591–9596.
Kim, J., K. Johnson, H. J. Chen, S. Carroll, and A. Laughon, 1997 *Drosophila* Mad binds to DNA and directly mediates activation of *vestigial* by Decapentaplegic. Nature 388: 304–308.
Koelzer, S., and T. Klein, 2006 Regulation of expression of Vg and establishment of the dorsoventral compartment boundary in the wing imaginal disc by Suppressor of Hairless. Dev. Biol. 289: 77–90.
Koide, R., S. Kobayashi, T. Shimohata, T. Ikeuchi, M. Maruyama *et al.*, 1999 A neurological disease caused by an expanded CAG trinucleotide repeat in the TATA-binding protein gene: a new polyglutamine disease? Hum. Mol. Genet. 8: 2047–2053.
Kornberg, T., 1981 Engrailed: a gene controlling compartment and segment formation in Drosophila. Proc. Natl. Acad. Sci. USA 78: 1095–1099.
Kovall, R. A., 2007 Structures of CSL, Notch and Mastermind proteins: piecing together an active transcription complex. Curr. Opin. Struct. Biol. 17: 117–127.
Langley, C. H., K. Stevens, C. Cardeno, Y. C. G. Lee, D. R. Schrider *et al.*, 2012 Genomic variation in natural populations of *Drosophila melanogaster*. Genetics 192: 533–598.
Langley, S. A., G. H. Karpen, and C. H. Langley, 2014 Nucleosomes shape DNA polymorphism and divergence. PLoS Genet. 10: 25–27.
Lawrence, P. A., and G. Morata, 1976 Compartments in the wing of *Drosophila*: a study of the *engrailed* gene. Dev. Biol. 50: 321–337.
Lawrence, P. A., G. Struhl, and G. Morata, 1979 Bristle patterns and compartment boundaries in the tarsi of *Drosophila*. J. Embryol. Exp. Morphol. 51: 195–208.
Lecourtois, M., and F. Schweisguth, 1995 The neurogenic suppressor of hairless DNA-binding protein mediates the transcriptional activation of the enhancer of split complex genes triggered by Notch signaling. Genes Dev. 9: 2598–2608.
Lewis, E. B., 1978 A gene complex controlling segmentation in *Drosophila*. Nature 276: 565–570.
Lin, Q., Q. Chen, L. Lin, S. Smith, and J. Zhou, 2007 Promoter targeting sequence mediates enhancer interference in the *Drosophila* embryo. Proc. Natl. Acad. Sci. USA 104: 3237–3242.
Liu, F., and J. W. Posakony, 2012 Role of architecture in the function and specificity of two notch-regulated transcriptional enhancer modules. PLoS Genet. 8: e1002796.
Lowary, P. T., and J. Widom, 1998 New DNA sequence rules for high affinity binding to histone octamer and sequence-directed nucleosome positioning. J. Mol. Biol. 276: 19–42.
Maier, D., P. Kurth, A. Schulz, A. Russell, Z. Yuan *et al.*, 2011 Structural and functional analysis of the repressor complex in the Notch signaling pathway of *Drosophila melanogaster*. Mol. Biol. Cell 22: 3242–3252.
Markstein, M., R. Zinzen, P. Markstein, K.-P. Yee, A. Erives *et al.*, 2004 A regulatory code for neurogenic gene expression in the *Drosophila* embryo. Development 131: 2387–2394.
Mathelier, A., O. Fornes, D. J. Arenillas, C. Y. Chen, G. Denay *et al.*, 2016 JASPAR 2016: a major expansion and update of the open-access database of transcription factor binding profiles. Nucleic Acids Res. 44: D110–D115.
Matsuda, S., J. Blanco, and O. Shimmi, 2013 A feed-forward loop coupling extracellular BMP transport and morphogenesis in *Drosophila* wing. PLoS Genet. 9: e1003403.
Mavrich, T. N., C. Jiang, I. P. Ioshikhes, X. Li, B. J. Venters *et al.*, 2008 Nucleosome organization in the *Drosophila* genome. Nature 453: 358–362.
McGinnis, W., M. S. Levine, E. Hafen, A. Kuroiwa, and W. J. Gehring, 1984 A conserved DNA sequence in homoeotic

genes of the Drosophila Antennapedia and bithorax complexes. Nature 308: 428–433.
Mukherjee, S., M. Thomas, N. Dadgar, A. P. Lieberman, and J. A. Iñiguez-Lluhí, 2009 Small ubiquitin-like modifier (SUMO) modification of the androgen receptor attenuates polyglutamine-mediated aggregation. J. Biol. Chem. 284: 21296–21306.
Nègre, N., C. D. Brown, L. Ma, C. A. Bristow, S. W. Miller *et al.*, 2011 A *cis*-regulatory map of the *Drosophila* genome. Nature 471: 527–531.
Neumann, C. J., and S. M. Cohen, 1996a A hierarchy of cross-regulation involving Notch, wingless, vestigial and cut organizes the dorsal/ventral axis of the Drosophila wing. Development 122: 3477–3485.
Neumann, C. J., and S. M. Cohen, 1996b Distinct mitogenic and cell fate specification functions of wingless in different regions of the wing. Development 122: 1781–1789.
Newfeld, S. J., A. T. Schmid, and B. Yedvobnick, 1993 Homopolymer length variation in the *Drosophila* gene *mastermind*. J. Mol. Evol. 37: 483–495.
Newfeld, S. J., E. H. Chartoff, J. M. Graff, D. A. Melton, and W. M. Gelbart, 1996 Mothers against dpp encodes a conserved cytoplasmic protein required in DPP/TGF-beta responsive cells. Development 122: 2099–2108.
Newfeld, S. J., A. Mehra, M. A. Singer, J. L. Wrana, L. Attisano *et al.*, 1997 Mothers against dpp participates in a DDP/TGF-beta responsive serine-threonine kinase signal transduction cascade. Development 124: 3167–3176.
Nien, C.-Y., H.-L. Liang, S. Butcher, Y. Sun, S. Fu *et al.*, 2011 Temporal coordination of gene networks by Zelda in the early *Drosophila* embryo. PLoS Genet. 7: e1002339.
Noyes, M. B., X. Meng, A. Wakabayashi, S. Sinha, M. H. Brodsky *et al.*, 2008 A systematic characterization of factors that regulate *Drosophila* segmentation via a bacterial one-hybrid system. Nucleic Acids Res. 36: 2547–2560.
O'Connor, M. B., D. Umulis, H. G. Othmer, and S. S. Blair, 2006 Shaping BMP morphogen gradients in the *Drosophila* embryo and pupal wing. Development 133: 183–193.
Ozdemir, A., L. Ma, K. P. White, and A. Stathopoulos, 2014 Su (H)-mediated repression positions gene boundaries along the dorsal-ventral axis of *Drosophila* embryos. Dev. Cell 31: 100–113.
Perez, M. K., H. L. Paulson, S. J. Pendse, S. J. Saionz, N. M. Bonini *et al.*, 1998 Recruitment and the role of nuclear localization in polyglutamine-mediated aggregation. J. Cell Biol. 143: 1457–1470.
Perry, M. W., A. N. Boettiger, and M. Levine, 2011 Multiple enhancers ensure precision of gap gene-expression patterns in the *Drosophila* embryo. Proc. Natl. Acad. Sci. USA 108: 13570–13575.
Perutz, M. F., J. T. Finch, J. Berriman, and A. Lesk, 2002a Amyloid fibers are water-filled nanotubes. Proc. Natl. Acad. Sci. USA 99: 5591–5595.
Perutz, M. F., B. J. Pope, D. Owen, E. E. Wanker, and E. Scherzinger, 2002b Aggregation of proteins with expanded glutamine and alanine repeats of the glutamine-rich and asparagine-rich domains of Sup35 and of the amyloid β-peptide of amyloid plaques. Proc. Natl. Acad. Sci. USA 99: 5596–5600.
Raftery, L. A., V. Twombly, K. Wharton, and W. M. Gelbart, 1995 Genetic screens to identify elements of the decapentaplegic signaling pathway in Drosophila. Genetics 139: 241–254.
Ratnaparkhi, G. S., H. A. Duong, and A. J. Courey, 2008 Dorsal interacting protein 3 potentiates activation by *Drosophila* Rel homology domain proteins. Dev. Comp. Immunol. 32: 1290–1300.
Restrepo, S., J. J. Zartman, and K. Basler, 2014 Coordination of patterning and growth by the morphogen DPP. Curr. Biol. 24: R245–R255.
Rice, C., D. Beekman, L. Liu, and A. Erives, 2015 The nature, extent, and consequences of genetic variation in the *opa* repeats of *Notch* in *Drosophila*. G3 (Bethesda) 5: 2405–2419.
Russo, M. W., B. R. Sevetson, and J. Milbrandt, 1995 Identification of NAB1, a repressor of NGFI-A- and Krox20-mediated transcription. Proc. Natl. Acad. Sci. USA 92: 6873–6877.
Sandelin, A., W. Alkema, P. Engström, W. W. Wasserman, and B. Lenhard, 2004 JASPAR: an open-access database for eukaryotic transcription factor binding profiles. Nucleic Acids Res. 32: D91–D94.
Sasaki, H., and B. L. Hogan, 1996 Enhancer analysis of the mouse HNF-3 beta gene: regulatory elements for node/notochord and floor plate are independent and consist of multiple subelements. Genes Cells 1: 59–72.
Schaaf, C. A., Z. Misulovin, M. Gause, A. Koenig, and D. Dorsett, 2013 The Drosophila *Enhancer of split* gene complex: architecture and coordinate regulation by Notch, Cohesin, and Polycomb group proteins. G3 (Bethesda) 3: 1785–1794.
Schroeter, E. H., J. A. Kisslinger, and R. Kopan, 1998 Notch-1 signalling requires ligand-induced proteolytic release of intracellular domain. Nature 393: 382–386.
Schuldt, J., and H. Brand, 1999 Mastermind acts downstream of notch to specify neuronal cell fates in the *Drosophila* central nervous system. Dev. Biol. 205: 287–295.
Schweisguth, F., 1995 Suppressor of Hairless is required for signal reception during lateral inhibition in the Drosophila pupal notum. Development 121: 1875–1884.
Segal, E., and J. Widom, 2009 Poly(dA:dT) tracts: major determinants of nucleosome organization. Curr. Opin. Struct. Biol. 19: 65–71.
Segal, E., Y. Fondufe-Mittendorf, L. Chen, A. Thåström, Y. Field *et al.*, 2006 A genomic code for nucleosome positioning. Nature 442: 772–778.
Sekelsky, J. J., S. J. Newfeld, L. A. Raftery, E. H. Chartoff, and W. M. Gelbart, 1995 Genetic characterization and cloning of mothers against dpp, a gene required for decapentaplegic function in Drosophila melanogaster. Genetics 139: 1347–1358.
Slattery, M., R. Voutev, L. Ma, N. Nègre, K. P. White *et al.*, 2013 Divergent transcriptional regulatory logic at the intersection of tissue growth and developmental patterning. PLoS Genet. 9: e1003753.
Staudt, N., S. Fellert, H.-R. Chung, H. Jäckle, and G. Vorbrüggen, 2006 Mutations of the *Drosophila* zinc finger-encoding gene *vielfältig* impair mitotic cell divisions and cause improper chromosome segregation. Mol. Biol. Cell 17: 2356–2365.
Steneberg, P., J. Hemphala, and C. Samakovlis, 1999 Dpp and Notch specify the fusion cell fate in the dorsal branches of the *Drosophila* trachea. Mech. Dev. 87: 153–163.
Svaren, J., B. R. Sevetson, E. D. Apel, D. B. Zimonjic, N. C. Popescu *et al.*, 1996 NAB2, a corepressor of NGFI-A (Egr-1) and Krox20, is induced by proliferative and differentiative stimuli. Mol. Cell. Biol. 16: 3545–3553.
Syed, S. H., D. Goutte-Gattat, N. Becker, S. Meyer, M. S. Shukla *et al.*, 2010 Single-base resolution mapping of H1-nucleosome interactions and 3D organization of the nucleosome. Proc. Natl. Acad. Sci. USA 107: 9620–9625.
Tanimoto, H., S. Itoh, P. ten Dijke, and T. Tabata, 2000 Hedgehog creates a gradient of DPP activity in *Drosophila* wing imaginal discs. Mol. Cell 5: 59–71.
Terriente Félix, J., M. Magariños, and F. J. Díaz-Benjumea, 2007 Nab controls the activity of the zinc-finger transcription factors Squeeze and Rotund in *Drosophila* development. Development 134: 1845–1852.
Thåström, A., P. T. Lowary, H. R. Widlund, H. Cao, M. Kubista *et al.*, 1999 Sequence motifs and free energies of selected natural and non-natural nucleosome positioning DNA sequences. J. Mol. Biol. 288: 213–229.

Tóth-Petróczy, Á., C. J. Oldfield, I. Simon, Y. Takagi, A. K. Dunker *et al.*, 2008 Malleable machines in transcription regulation: the Mediator complex. PLOS Comput. Biol. 4: e1000243.

Tun, T., Y. Hamaguchi, N. Matsunami, T. Furukawa, T. Honjo *et al.*, 1994 Recognition sequence of a highly conserved DNA binding protein RBP-J kappa. Nucleic Acids Res. 22: 965–971.

van de Wetering, M., R. Cavallo, D. Dooijes, M. van Beest, J. van Es *et al.*, 1997 Armadillo coactivates transcription driven by the product of the Drosophila segment polarity gene *dTCF*. Cell 88: 789–799.

Vilella, A. J., J. Severin, A. Ureta-Vidal, L. Heng, R. Durbin *et al.*, 2009 EnsemblCompara GeneTrees: complete, duplication-aware phylogenetic trees in vertebrates. Genome Res. 19: 327–335.

Voas, M. G., and I. Rebay, 2004 Signal integration during development: insights from the *Drosophila* eye. Dev. Dyn. 229: 162–175.

Ward, E. J., H. R. Shcherbata, S. H. Reynolds, K. A. Fischer, S. D. Hatfield *et al.*, 2006 Stem cells signal to the niche through the Notch pathway in the *Drosophila* ovary. Curr. Biol. 16: 2352–2358.

Weatherbee, S. D., H. Frederik Nijhout, L. W. Grunert, G. Halder, R. Galant *et al.*, 1999 Ultrabithorax function in butterfly wings and the evolution of insect wing patterns. Curr. Biol. 9: 109–115.

Weiss, A., E. Charbonnier, E. Ellertsdóttir, A. Tsirigos, C. Wolf *et al.*, 2010 A conserved activation element in BMP signaling during *Drosophila* development. Nat. Struct. Mol. Biol. 17: 69–76.

Wharton, K. A., B. Yedvobnick, V. G. Finnerty, and S. Artavanis-Tsakonas, 1985 *opa*: a novel family of transcribed repeats shared by the *Notch* locus and other developmentally regulated loci in D. melanogaster. Cell 40: 55–62.

Wiersdorff, V., T. Lecuit, S. M. Cohen, and M. Mlodzik, 1996 *Mad* acts downstream of Dpp receptors, revealing a differential requirement for *dpp* signaling in initiation and propagation of morphogenesis in the *Drosophila* eye. Development 122: 2153–2162.

Williams, J. A., S. W. Paddock, K. Vorwerk, and S. B. Carroll, 1994 Organization of wing formation and induction of a wing-patterning gene at the dorsal/ventral compartment boundary. Nature 368: 299–305.

Wisotzkey, R. G., A. Mehra, D. J. Sutherland, L. L. Dobens, X. Liu *et al.*, 1998 Medea is a Drosophila Smad4 homolog that is differentially required to potentiate DPP responses. Development 125: 1433–1445.

Yedvobnick, B., D. Smoller, P. Young, and D. Mills, 1988 Molecular analysis of the neurogenic locus mastermind of Drosophila melanogaster. Genetics 118: 483–497.

Zhu, L. J., R. G. Christensen, M. Kazemian, C. J. Hull, M. S. Enuameh *et al.*, 2011 FlyFactorSurvey: a database of *Drosophila* transcription factor binding specificities determined using the bacterial one-hybrid system. Nucleic Acids Res. 39: D111–D117.

Zhu, Q., and M. S. Halfon, 2007 Vector-dependent gene expression driven by insulated P-element reporter vectors. Fly (Austin) 1: 55–56.

Ziv, O., Y. Suissa, H. Neuman, T. Dinur, P. Geuking *et al.*, 2009 The co-regulator dNAB interacts with Brinker to eliminate cells with reduced Dpp signaling. Development 136: 1137–1145.

Communicating editor: J. A. Birchler

GENETICS

Supporting Information
www.genetics.org/lookup/suppl/doi:10.1534/genetics.116.186791/-/DC1

Integration of Orthogonal Signaling by the Notch and Dpp Pathways in *Drosophila*

Elizabeth Stroebele and Albert Erives

DOI: 10.1534/genetics.116.186791

Figure S1.

Source derivation of IUPAC consensus motifs.

As explained in the Material and Methods section, IUPAC motifs were derived from various genomic data sets from the literature and/or transcription factor databases (JASPAR, FlyFactorSurvey). To mutate the three Mad sites in the *nab* DWME (*nab-A* fragment), the prominent CG dinucleotide at positions 10 and 11 were mutated to T's.

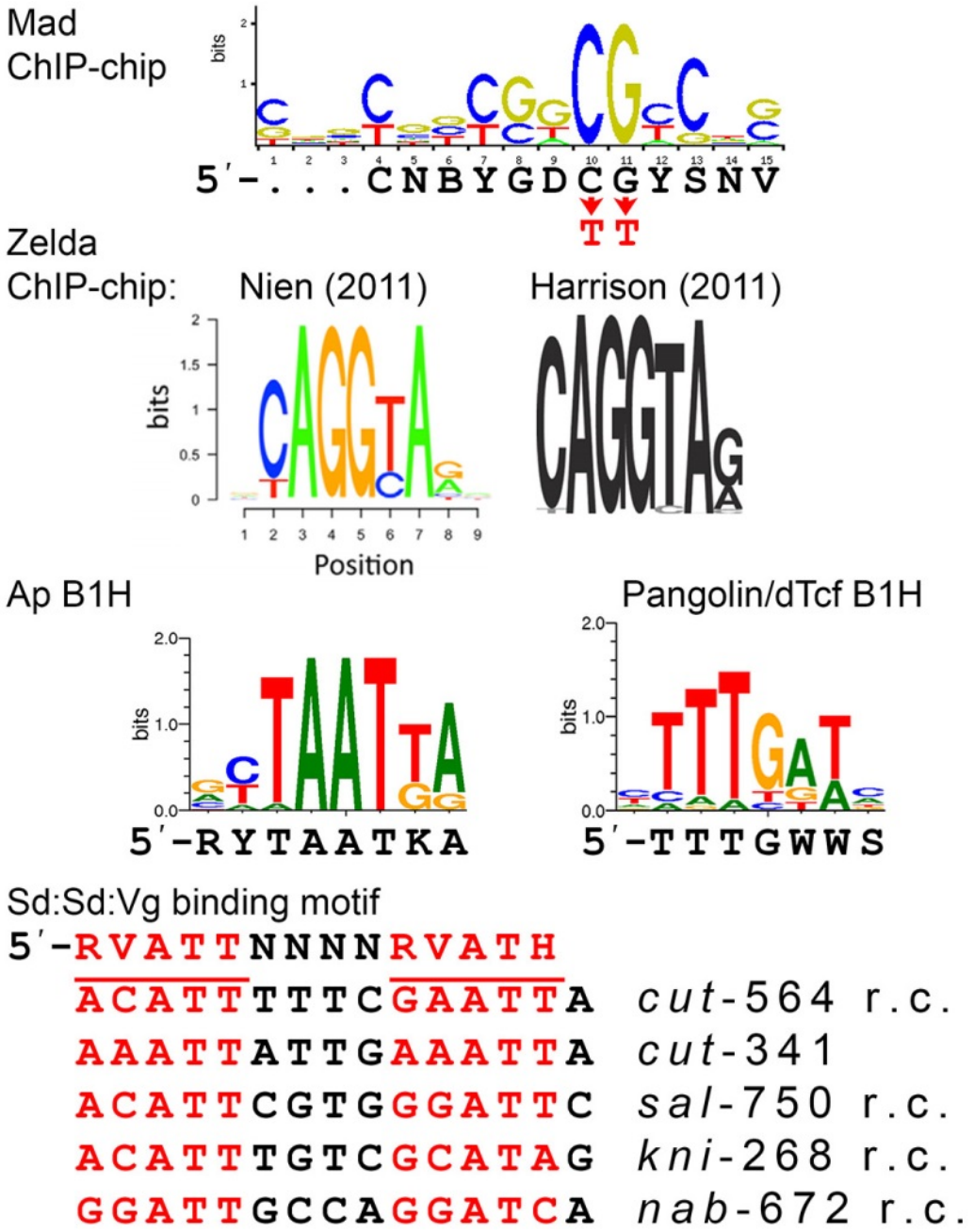

Figure S2.

Beta-galactosidase staining for 7 independent P-element lines carrying *nab-A-lacZ.*

Shown are dissected late third instar discs stained over night in X-gal staining solution. Discs were dissected from either control untransformed w^{1118} flies **(A)** or w^{1118} flies carrying one of seven different P-element integrations **(B)**.

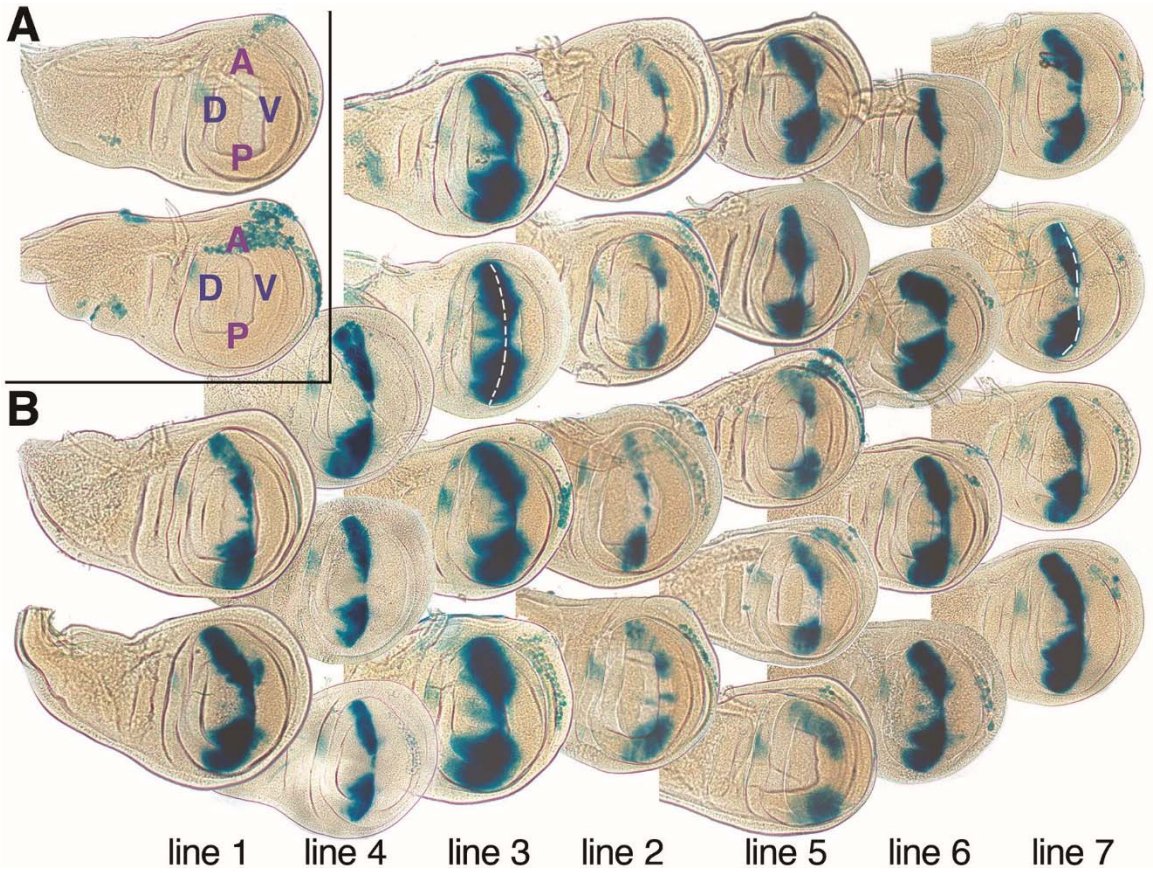

Figure S3.

Live GFP activity driven by the *nab-A* dorsal wing margin enhancer.

Live GFP florescence in dissected wing imaginal disc of late third instar larva (A darkfield, and B brightfield), a wandering stage third instar larva with insets showing both wing discs oriented for comparison (C), and of pupal stages (D). Arrows in (D) point to GFP signal along wing margin (black arrows) and in the haltere (white arrow).

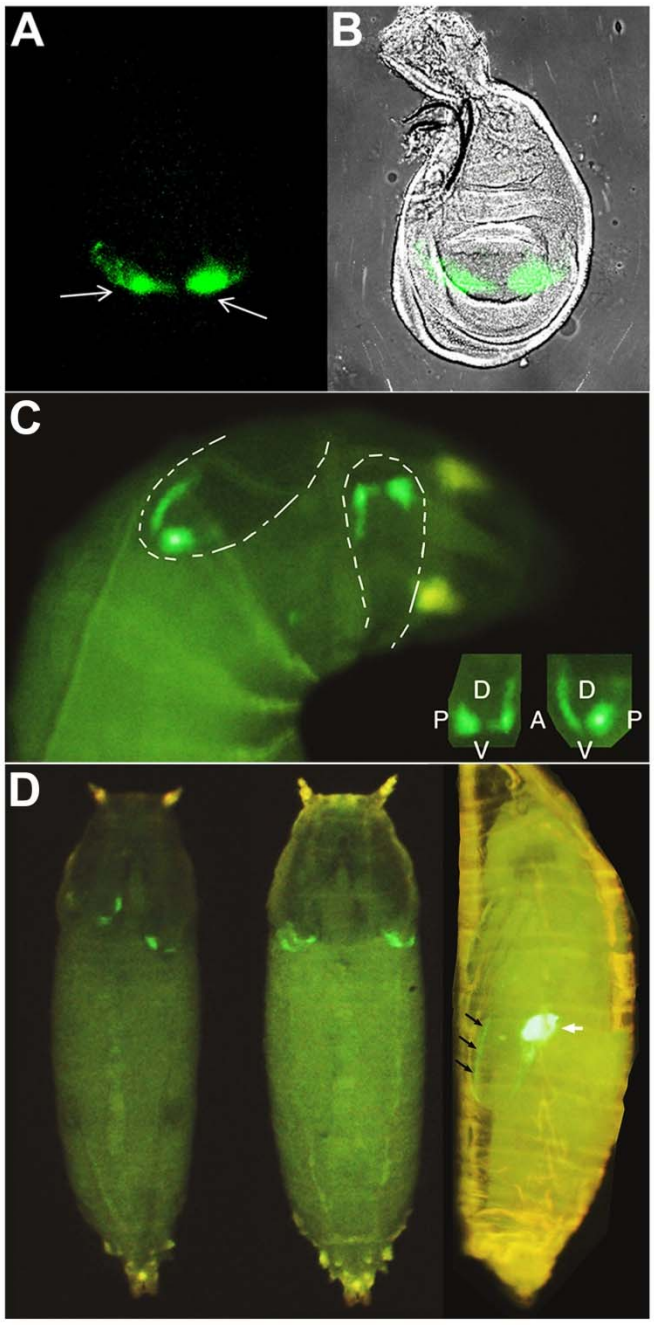

Figure S4. Default fixed nucleosomal positions in the *nab* DWME.

Shown are embryonic stage 5 fixed nucleosomal positions over the *nab-DAB* region starting at the *nab-D* fragment (nucleosomal data from Langley, Karpen, and Langley 2014). Highlighted are sequences matching Apterous (blue) and Su(H) (red in yellow highlight) binding motifs, and nucleosomal positions (underlining). With these default fixed nucleosomal positions, the central and key Su(H) site S1 is predicted to be unavailable for binding. In this regard, it is interesting to note that many of the Apterous sites coincide with nucleosomal DNA entry positions, where linker histone H1 typically binds. Thus, Apterous may possibly play a role in promoting alternate nucleosomal positions, which make the Su(H) site available. Two panels are shown for increased clarity in depicting alternate nucleosome positions. **(A)** Shown are fixed nucleosomal positions 1a, 1b, 2a, and 3. Positions 1a and 1b are partially overlapping (double-underlining). **(B)** Shown are fixed nucleosomal positions 1c, 2b, and 3. Positions 1a and 1b (panel A) overlap with 1c (panel B). Position 2a (panel A) overlaps with position 2b (panel B).

A

CTCATATGTATCTTTTCATTTTAAATATATTATATGTATATAGAGATATATAGATCATAAACTTTCACTAAAACTGGCCA
AATGTGTCTATTATAACCCTCTCATTAACTAGTTTTAATAACCTTGTCACTTAGCTACTAGTTTGCTGGATTTAGCGTAC
ATTTATAAGCACTTTCAAAGTCGACACTAATTTCAGTCCAGTTCAGCTCAGTTGATCACAGCTTTCAAGTGGACGCAACT
GGTCTGATATTTTAGTTTCCAAACTATTTATGATATACCCAATTAAGCGGCTAAGAATGCGAATTATTCTTGCTGCCTGG
CCATAAATCGCAACAACCCCATGGAGCGGAGCGTGGGTTAATGGCGCGAAGTGCGCATCCTTGGTGTTGCACGTCGGTGG
ATGCGCTTGTGGCTTCCAGTTGGCCAAGGCAACTGAATACAAACCACAAAAAAAAAAACAGAGCGAGTGGAATCGGAGGA
TGGCAATCGATGTAGGCAGCTTTTTCTGCCCTGAGTTTGTTATAATTTAGCCGACCAGCTCGTTTTTCTATTAATTAAAG
CTGGCTGCAGACGTTGTCGCCGCCTGAAATATTCTCACATAATTATTTACGATTTGACATAATCATCATCCTCGTCATCG
GCGTCGTCCATTTAGAGCTGTGCTGCCATAACAGTTACAGTCTCCTCGATCGGGGGATTCATTAGTATGAGCAATAAATC
GCTGGCTAGTCAGGATGGTTTCCTATGAACTTGAGTGTAGGTACGACTTTATATGTATGTACATATATATTTCACACGAT
GCCATCCCATATACCCATGAAAATTTACCTATTTTGAGCCAAAAATTGAAAGTGATAAAAGCAAACAAAAAAAAAGAGAG
AATAGGTTAGATTTAAATGATGATCCTGGCAATCCTTGCTGGCATCTTGCGCATGCGTGACGCATTTCTAACGAGTTTGC
CGACTCAAAGCGGATCGTATCGCATCCTTGGTCTTTCAGAAGGGGTTGAACCACCATGCTTATGCAGATGAGTTGGTTCC
CAGCTCTTGCCTCATCCTTTTTGTGTGCTTTCGAGTTTTTTTTTTTTGCTCTGCTCAGCCTCTACGAAAAAAGGGTTAGG
GTCCAGACGTCCGTCGAGTTTTTTTTTTTTTTTGGGTAAGAAAAAGCGAATTTAATTAAAATTTTTTTCTTATAGGCGCG
TAGCATTGTGAGAACGTCGCAGGCCAGAACTTAATAAATATCATTTTTTGCTGGAACTTCTTCAAGCCAGTTTCTTATGC
ATACG

B

CTCATATGTATCTTTTCATTTTAAATATATTATATGTATATAGAGATATATAGATCATAAACTTTCACTAAAACTGGCCA
AATGTGTCTATTATAACCCTCTCATTAACTAGTTTTAATAACCTTGTCACTTAGCTACTAGTTTGCTGGATTTAGCGTAC
ATTTATAAGCACTTTCAAAGTCGACACTAATTTCAGTCCAGTTCAGCTCAGTTGATCACAGCTTTCAAGTGGACGCAACT
GGTCTGATATTTTAGTTTCCAAACTATTTATGATATACCCAATTAAGCGGCTAAGAATGCGAATTATTCTTGCTGCCTGG
CCATAAATCGCAACAACCCCATGGAGCGGAGCGTGGGTTAATGGCGCGAAGTGCGCATCCTTGGTGTTGCACGTCGGTGG
ATGCGCTTGTGGCTTCCAGTTGGCCAAGGCAACTGAATACAAACCACAAAAAAAAAAACAGAGCGAGTGGAATCGGAGGA
TGGCAATCGATGTAGGCAGCTTTTTCTGCCCTGAGTTTGTTATAATTTAGCCGACCAGCTCGTTTTTCTATTAATTAAAG
CTGGCTGCAGACGTTGTCGCCGCCTGAAATATTCTCACATAATTATTTACGATTTGACATAATCATCATCCTCGTCATCG
GCGTCGTCCATTTAGAGCTGTGCTGCCATAACAGTTACAGTCTCCTCGATCGGGGGATTCATTAGTATGAGCAATAAATC
GCTGGCTAGTCAGGATGGTTTCCTATGAACTTGAGTGTAGGTACGACTTTATATGTATGTACATATATATTTCACACGAT
GCCATCCCATATACCCATGAAAATTTACCTATTTTGAGCCAAAAATTGAAAGTGATAAAAGCAAACAAAAAAAAAGAGAG
AATAGGTTAGATTTAAATGATGATCCTGGCAATCCTTGCTGGCATCTTGCGCATGCGTGACGCATTTCTAACGAGTTTGC
CGACTCAAAGCGGATCGTATCGCATCCTTGGTCTTTCAGAAGGGGTTGAACCACCATGCTTATGCAGATGAGTTGGTTCC
CAGCTCTTGCCTCATCCTTTTTGTGTGCTTTCGAGTTTTTTTTTTTTGCTCTGCTCAGCCTCTACGAAAAAAGGGTTAGG
GTCCAGACGTCCGTCGAGTTTTTTTTTTTTTTTGGGTAAGAAAAAGCGAATTTAATTAAAATTTTTTTCTTATAGGCGCG
TAGCATTGTGAGAACGTCGCAGGCCAGAACTTAATAAATATCATTTTTTGCTGGAACTTCTTCAAGCCAGTTTCTTATGC
ATACG

File S1: FASTA sequences. (.txt, 4 KB)

Available for download as a .txt file at:

http://www.genetics.org/lookup/suppl/doi:10.1534/genetics.116.186791/-/DC1/FileS1.txt

Supporting File S2. Sequence alignment of clones from the *nab* intronic enhancer complex. Indicated are the primers used (underlined) as well as sequence differences between clones. “REF” corresponds to the *iso-1* reference genome sequence. BAC and w1118 correspond to genomic sources for PCR amplified fragments (see Material and Methods for details). Gray shaded sequences correspond to un-sequenced regions and/or sequences inferred from sequencing clones amplified from the same source.

```
           C-fwd primer
CDAB_REF   ACAAGTACAATGGACATGGCGAAACAGGTCCTATTAAAACCCTCAAATTGGCAAGATTAA
CDAB_BAC   ACAAGTACAATGGACATGGCGAAACAGGTCCTATTAAAACCCTCAAATTGGCAAGATTAA
CDA_BAC    ACAAGTACAATGGACATGGCGAAACAGGTCCTATTAAAACCCTCAAATTGGCAAGATTAA
C_w1118    ACAAGTACAATGGACATGGCGAAACAGGTCCTATTAAAACC-TCAAATTGGCAAGATTAA

CDAB_REF   GATCGTAATGACCCCGAAAATAATGCACTTAATATTTTGGACAGACATTATTCTTTTCCT
CDAB_BAC   GATCGTAATGACCCCGAAAATAATGCACTTAATATTTTGGACAGACATTATTCTTTTCCT
CDA_BAC    GATCGTAATGACCCCGAAAATAATGCACTTAATATTTTGGACAGACATTATTCTTTTCCT
C_w1118    GATCGTAATGACCCCGAAAATAATGCACTTAATATTTTGGACAGACATTATTCTTTTCCT

CDAB_REF   GTGCAGGTTATGGTTATGGTTCCTCTGCCGGGGCCATTGGCCATTGGCACGTACGGTCCA
CDAB_BAC   GTGCAGGTTATGGTTATGGTTCCTCTGCCGGGGCCATTGGCCATTGGCACGTACGGTCCA
CDA_BAC    GTGCAGGTTATGGTTATGGTTCCTCTGCCGGGGCCATTGGCCATTGGCACGTACGGTCCA
C_w1118    GTGCAGGTTATGGTTATGGTTCCTCTGCCGGGGCCATTGGCCATTGGCACGTACGGTCCA

CDAB_REF   CGTTATTGCCACCAATGGAATTTTGATCGACAAGAATTTGGTCGTTGAAAAAGTTGGCTT
CDAB_BAC   CGTTATTGCCACCAATGGAATTTTGATCGACAAGAATTTGGTCGTTGAAAAAGTTGGCTT
CDA_BAC    CGTTATTGCCACCAATGGAATTTTGATCGACAAGAATTTGGTCGTTGAAAAAGTTGGCTT
C_w1118    CGTTATTGCCACCAATGGAATTTTGATCGACAAGAATTTGGTCGTTGAAAAAGTTGGCTT

CDAB_REF   TTAATTTATCGTTGTATATGAGAAATAGTTTCGGTTACTTGCCCATTGCCGATGCCAAGC
CDAB_BAC   TTAATTTATCGTTGTATATGAGAAATAGTTTCGGTTACTTGCCCATTGCCGATGCCAAGC
CDA_BAC    TTAATTTATCGTTGTATATGAGAAATAGTTTCGGTTACTTGCCCATTGCCGATGCCAAGC
C_w1118    TTAATTTATCGTTGTATATGAGAAATAGTTTCGGTTACTTGCCCATTGCCGATGCCAAGC

C_w1118    AGAAAGGGAGGATCGAATGGAGGAGGAGGAGGAGGATTCAGACCCTGGTCCCAGTCCCAA
CDAB_REF   AGAAAGGGAGGATCGAATGGAGGAGGAGGAGGAGGATTCAGACCCTGGTCCCAGTCCCAA
CDAB_BAC   AGAAAGGGAGGATCGAATGGAGGAGGAGGAGGAGGATTCAGACCCTGGTCCCAGTCCCAA
CDA_BAC    AGAAAGGGAGGATCGAATGGAGGAGGAGGAGGAGGATTCAGACCCTGGTCCCAGTCCCAA

CDAB_REF   GTCCCAGGTTCCAGGTTCCAGGTTCCGATTCCAGGTCCAACTCTCCAAGTCAAAGTCTGC
CDAB_BAC   GTCCCAGGTTCCAGGTTCCAGGTTCCGATTCCAGGTCCAACTCTCCAAGTCAAAGTCTGC
CDA_BAC    GTCCCAGGTTCCAGGTTCCAGGTTCCGATTCCAGGTCCAACTCTCCAAGTCAAAGTCTGC
C_w1118    GTCCCAGGTTCCAGGTTCCAGGTTCCGATTCCAGGCCCAACTCTCCAAGTCAAAGTCTGC

CDAB_REF   AAAGTCCGGCGTCTACTTTTTGCCCATAATCGAAGCGATCGCACGATTGACTGCTCCGCT
CDAB_BAC   AAAGTCCGGCGTCTACTTTTTGCCCATAATCGAAGCGATCGCACGATTGACTGCTCCGCT
CDA_BAC    AAAGTCCGGCGTCTACTTTTTGCCCATAATCGAAGCGATCGCACGATTGACTGCTCCGCT
C_w1118    AAAGTCCGGCGTCTACTTTTTGCCCATAATCGAAGCGATCGCACGATTGACTGCTCCGCT

CDAB_REF   CCACACGCACACACAGACCGCTCACACACACACACACATGCACTATAACGCATTTTCTAA
CDAB_BAC   CCACACGCACACACAGACCGCTCACACACACACACACATGCACTATAACGCATTTTCTAA
CDA_BAC    CCACACGCACACACAGACCGCTCACACACACACACACATGCACTATAACGCATTTTCTAA
C_w1118    CCACACGCACACACAGACCGCTCACACACACACACACATGCACTATAACGCATTTTCTAA

CDAB_REF   ATGCACTGTGAGAAAAGTGTGTCAAAATAATACAAATAATATAGGCATGAGCGAGGTACA
CDAB_BAC   ATGCACTGTGAGAAAAGTGTGTCAAAATAATACAAATAATATAGGCATGAGCGAGGTACA
CDA_BAC    ATGCACTGTGAGAAAAGTGTGTCAAAATAATACAAATAATATAGGCATGAGCGAGGTACA
C_w1118    ATGCACTGTGAGAAAAGTGTGTCAAAATAATACAAATAATATAGGCATGAGCGAGGTACA
```

```
CDAB_REF  TACTTAACTTAATGCTCAGAGACGCCTTGTATGAAATATATATAATTATAATTTCCATTA
CDAB_BAC  TACTTAACTTAATGCTCAGAGACGCCTTGTATGAAATATATATAATTATAATTTCCATTA
CDA_BAC   TACTTAACTTAATGCTCAGAGACGCCTTGTATGAAATATATATAATTATAATTTCCATTA
C_w1118   TACTTAACTTAATGCTCAGAGACGCCTTGTATGAAATATATATAATTATAATTTCCATTA

CDAB_REF  GAAACAATTATCACATCTTATCAGAATCAACCACACTTTTTTTCTAAGTGCCTATCCTGC
CDAB_BAC  GAAACAATTATCACATCTTATCAGAATCAACCACACTTTTTTTCTAAGTGCCTATCCTGC
CDA_BAC   GAAACA-TTATCACATCTTATCAGAATCAACCACACTTTTTTTCTAAGTGCCTATCCTGC
C_w1118   GAAACAATTATCACATCTTATCAGAATCAACCACACTTTTTTTCTAAGTGCCTATCCTGC

CDAB_REF  TGGCTGCTCGCGGTTTTCCGTTTTCTGCTCCTGGCTGCTTGGGCAGCTGCTTGGTATGTG
CDAB_BAC  TGGCTGCTCGCGGTTTTCCGTTTTCTGCTCCTGGCTGCTTGGGCAGCTGCTTGGTATGTG
CDA_BAC   TGGCTGCTCGCGGTTTTCCGTTTTCTGCTCCTGGCTGCTTGGGCAGCTGCTTGGTATGTG
C_w1118   TGGCTGCTCGCGGTTTTCCGTTTTCTGCTCCTGGCTGCTTGGGCAGCTGCTTGGTATGTG

CDAB_REF  GCGTCGAATGTCATTATTGCTGCCAAGTGCCAACTAAAAAGTTACTGCAGTTAATTTTTT
CDAB_BAC  GCGTCGAATGTCATTATTGCTGCCAAGTGCCAACTAAAAAGTTACTGCAGTTAATTTTTT
CDA_BAC   GCGTCGAATGTCATTATTGCTGCCAAGTGCCAACTAAAAAGTTACTGCAGTTAATTTTTT
C_w1118   GCGTCGAATGTCATTATTGCTGCCAAGTGCCAACTAAAAAGTTACTGCAGTTAATTTTTT

CDAB_REF  GTCCATCTTCACCATTTGCCGTTCGCATAAAAACAGCATATTTAGCAAATGACAACAACA
CDAB_BAC  GTCCATCTTCACCATTTGCCGTTCGCATAAAAACAGCATATTTAGCAAATGACAACAACA
CDA_BAC   GTCCATCTTCACCATTTGCCGTTCGCATAAAAACAGCATATTTAGCAAATGACAACAACA
C_w1118   GTCCATCTTCACCATTTGCCGTTCGCATAAAAACAGCATATTTAGCAAATGACAACAACA

CDAB_REF  ACAGCAGCCGCAGCATCGGCTCTTACGCAGTGGGTAAAAAAAATGAAAGCAAGCAAAAAA
CDAB_BAC  ACAGCAGCCGCAGCATCGGCTCTTACGCAGTGGGTAAAAAAAATGAAAGCAAGCAAAAAA
CDA_BAC   ACAGCAGCCGCAGCATCGGCTCTTACGCAGTGGGTAAAAAAAATGAAAGCAAGCAAAAAA
C_w1118   ACAGCAGCCGCAGCATCGGCTCTTACGCAGTGGGTAAAAAAAATGAAAGCAAGCAAAAAA

CDAB_REF  AAAAAAGAAAACCAAACCCGCAAATTAAATAAATAAAAAATCAGCAACAATCCGCAGAA
CDAB_BAC  AAAAA-GAAAACCAAACCCGCAAATnnnnnnnnnnnnnnnnnnnnnnnnnnnnnnnn
CDA_BAC   AAAAA-GAAAACCAAACCCGCAAATnnnnnnnnnnnnnnnnnnnnnnnnnnnnnnnn
C_w1118   AAAAAAGAAAACCAAACCCGCAAATTAAATAAATAAAAAATCAGCAACAATCCGCAGAA

CDAB_REF  GCAGAGGAGCTGGAGCAGCCACAACAAAGTGTCCCCAGTTCTCCGCCTTCCC-AGCCTCC
CDAB_BAC  nnnnnnnnnnnnnnnnnnnnnnnnnnnnnnnnnnnnnnnnnnnnnnnnnnnnnnnnnnn
CDA_BAC   nnnnnnnnnnnnnnnnnnnnnnnnnnnnnnnnnnnnnnnnnnnnnnnnnnnnnnnnnnn
C_w1118   GCAGAGGAGCTGGAGCAGCCACAACAAAGTGTCCCCAGTTCTCCGC-TTCCCcAGCCTCC

CDAB_REF  CGCTTCGCCATATCCCCCCCGTTCCCCCC-ACCATTCACATTATTTGTGTATTGAAATCA
CDAB_BAC  nnnnnnnnnnnnnnnnnnnnnnnnnnnnnnnnnnnnnnnnnnnnnnnnnnnnnnnnnnn
CDA_BAC   nnnnnnnnnnnnnnnnnnnnnnnnnnnnnnnnnnnnnnnnnnnnnnnnnnnnnnnnnnn
C_w1118   CGCTctGCCATATCCCCCC-GTTCCaCCatACtATTCACATTATTTGTGTATTGAAATCA

CDAB_REF  CGTCTCATTTATTTATTGCTACCACCGGCTGCCCCTCTCCGTTTGCTCCACCAGACTCCC
CDAB_BAC  nnnnnnnnnnnnnnnnnnnnnnnnnnnnnnnnnnnnnnnnnnnnnnnnnnnnnnnnnnn
CDA_BAC   nnnnnnnnnnnnnnnnnnnnnnnnnnnnnnnnnnnnnnnnnnnnnnnnnnnnnnnnnnn
C_w1118   CGTCTCATTTATTTATTGCTACCACCGGCTGCCCCTCTCCGTTTGCTCCACCAGACTCCC
```

```
CDAB_REF   GACTTACGCAGGTCTGCGTTAAATACCCAAGTTAGGATCAGGGAGCGGGCGGTGGCAAGT
CDAB_BAC   nnnnnnnnnnnnnnnnnnnnnnnnnnnnnnnnnnnnnnnnnnnnnnnnnnnnnnnnnnnn
CDA_BAC    nnnnnnnnnnnnnnnnnnnnnnnnnnnnnnnnnnnnnnnnnnnnnnnnnnnnnnnnnnnn
C_w1118    GACTTACGCAGGTCTGCGTTAAATACCCAAGTTAGGATCgGGGAGCGGGCGGTGGCAAGT

CDAB_REF   GATGGAATAGACCAGAAGTGTGGCCACGCTCTTAACCCTTCAGCGGTCACTCTAGG----
CDAB_BAC   nnnnnnnnnnnnnnnnnnnnnnnnnnnnnnnnnnnnnnnnnnnnnnnnnnnnnnnnnnnn
CDA_BAC    nnnnnnnnnnnnnnnnnnnnnnnnnnnnnnnnnnnnnnnnnnnnnnnnnnnnnnnnnnnn
C_w1118    GATGGgATAGACCAGAAGTGTGGCCACGCTaTTAACCCTTCAGCGGTCACTCTAtGctgg

CDAB_REF   --------TTTTTTTTTCAATTTCAAGATCAATTGAAAATCTTAAGAAAGCTTTCAGAAA
CDAB_BAC   nnnnnnnnnnnnnnnnnnnnnnnnnnnnnnnnnnnnnnnnnnnnnnnnnnnnnnnnnnnn
CDA_BAC    nnnnnnnnnnnnnnnnnnnnnnnnnnnnnnnnnnnnnnnnnnnnnnnnnnnnnnnnnnnn
C_w1118    ataaagatTTTTTTTTTCAATTTCAAGATCAATTGAAAATCTTAAGAAAGCTTTCAGAAA

                 D-fwd primer
CDAB_REF   AGCATTACTCATATGTATCTTTTCATTTTAAATATATTATATGTATATAGAGATATATAG
 DAB_BAC       5'-CTCATATGTATCTTTTCATTTTAAATATATTATATGTATATAGAGATATATAG
 DA_BAC        5'-CTCATATGTATCTTTTCATTTTAAATATATTATATGTATATAGAGATATATAG
CDAB_BAC   nnnnnnnnnnnnnnnnnnnnnnnnATTTTAAATATATTATATGTATATAGAGATATATAG
CDA_BAC    nnnnnnnnnnnnnnnnnnnnnnnnATTTTAAATATATTATATGTATATAGAGATATATAG
C_w1118    AGCATTACTCATATGTATCTTTTC-3'
                    C-rev primer

CDAB_REF   ATCATAAACTTTCACTAAAACTGGCCAAATGTGTCTATTATAACCCTCTCATTAACTAG
DAB_BAC    ATCATAAACTTTCACTAAAACTGGCCAAATGTGTCTATTATAACCCTCTCATTAACTAG
DA_BAC     ATCATAAACTTTCACTAAAACTGGCCAAATGTGTCTATTATAACCCTCTCATTAACTAG
CDAB_BAC   ATCATAAACTTTCACTAAAACTGCCCAAATGTGTCTATTATAACCCTCTCATTAACTAG
CDA_BAC    ATCATAAACTTTCACTAAAACTGCCCAAATGTGTCTATTATAACCCTCTCATTAACTAG

CDAB_REF   TTTTAATAACCTTGTCACTTAGCTACTAGTTTGCTGGATTTAGCGTACATTTATAAGCAC
DAB_BAC    TTTTAATAACCTTGTCACTTAGCTACTAGTTTGCTGGATTTAGCGTACATTTATAAGCAC
DA_BAC     TTTTAATAACCTTGTCACTTAGCTACTAGTTTGCTGGATTTAGCGTACATTTATAAGCAC
CDAB_BAC   TTTTAATAACCTTGTCACTTAGCTACTAGTTTGCTGGATTTAGCGTACATTTATAAGCAC
CDA_BAC    TTTTAATAACCTTGTCACTTAGCTACTAGTTTGCTGGATTTAGCGTACATTTATAAGCAC

                                                                  A-fwd
CDAB_REF   TTTCAAAGTCGACACTAATTTCAGTCCAGTTCAGCTCAGTTGATCACAGCTTTCAAGTGG
 Ax_w1118                                                      5'-TGG
 A_w1118                                                       5'-TGG
 AB_BAC                                                        5'-TGG
DAB_BAC    TTTCAAAGTCGACACTAATTTCAGTCCAGTTCAGCTCAGTTGATCACAGCTTTCAAGTGG
DA_BAC     TTTCAAAGTCGACACTAATTTCAGTCCAGTTCAGCTCAGTTGATCACAGCTTTCAAGTGG
CDAB_BAC   TTTCAAAGTCGACACTAATTTCAGTCCAGTTCAGCTCAGTTGATCACAGCTTTCAAGTGG
CDA_BAC    TTTCAAAGTCGACACTAATTTCAGTCCAGTTCAGCTCAGTTGATCACAGCTTTCAAGTGG

         primer (cont.)
CDAB_REF   ACGCAACTGGTCTGATATTTTAGTTTCCAAACTATTTATGATATACCCAATTAAGCGGCT
Ax_w1118   ACGCAACTGGTCTGATATTTTAGTTTCCAAACTATTTATGATATACCCAATTAAGCGGCT
A_w1118    ACGCAACTGGTCTGATATTTTAGTTTCCAAACTATTTATGATATACCCAATTAAGCGGCT
AB_BAC     ACGCAACTGGTCTGATATTTTAGTTTCCAAACTATTTATGATATACCCAATTAAGCGGCT
DAB_BAC    ACGCAACTGGTCTGATATTTTAGTTTCCAAACTATTTATGATATACCCAATTAAGCGGCT
DA_BAC     ACGCAACTGGTCTGATATTTTAGTTTCCAAACTATTTATGATATACCCAATTAAGCGGCT
CDAB_BAC   ACGCAACTGGTCTGATATTTTAGTTTCCAAACTATTTATGATATACCCAATTAAGCGGCT
CDA_BAC    ACGCAACTGGTCTGATATTTTAGTTTCCAAACTATTTATGATATACCCAATTAAGCGGCT
```

```
CDAB_REF   AAGAATGCGAATTATTCTTGCTGCCTGGCCATAAATCGCAACAACCCCATGGAGCGGAGC
Ax_w1118   AAGAATGCGAATTATTCTTGCTGCCTGGCCATAAATCGCAACAACCCCATGGAGCGGAGC
A_w1118    AAGAATGCGAATTATTCTTGCTGCCTGGCCATAAATCGCAACAACCCCATGGAGCGGAGC
AB_BAC     AAGAATGCGAATTATTCTTGCTGCCTGGCCATAAATCGCAACAACCCCATGGAGCGGAGC
DAB_BAC    gAGAATGCGAATTATTCTTGCTGCCTGGCCATAAATCGCAACAACCCCATGGAGCGGAGC
DA_BAC     gAGAATGCGAATTATTCTTGCTGCCTGGCCATAAATCGCAACAACCCCATGGAGCGGAGC
CDAB_BAC   AAGAATGCGAATTATTCTTGCTGCCTGGCCATAAATCGCAACAACCCCATGGAGCGGAGC
CDA_BAC    AAGAATGCGAATTATTCTTGCTGCCTGGCCATAAATCGCAACAACCCCATGGAGCGGAGC

CDAB_REF   GTGGGTTAATGGCGCGAAGTGCGCATCCTTGGTGTTGCACGTCGGTGGATGCGCTTGTGG
Ax_w1118   GTGGGTTAATGGCGCGAAGTGCGCATCCTTGGTGTTGCACGTCGGTGGATGCGCTTGTGG
A_w1118    GTGGGTTAATGGCGCGAAGTGCGCATCCTTGGTGTTGCACGTCGGTGGATGCGCTTGTGG
AB_BAC     GTGGGTTAATGGCGCGAAGTGCGCATCCTTGGTGTTGCACGTCGGTGGATGCGCTTGTGG
CDA_BAC    GTGGGTTAATGGCGCGAAGTGCGCATCCTTGGTGTTGCACGTCGGTGGATGCGCTTGTGG
CDAB_BAC   GTGGGTTAATGGCGCGAAGTGCGCATCCTTGGTGTTGCACGTCGGTGGATGCGCTTGTGG
DAB_BAC    GTGGGTTAATGGCGCGAAGTGCGCATCCTTGGTGTTGCACGTCGGTGGATGCGCTTGTGG
DA_BAC     GTGGGTTAATGGCGCGAAGTGCGCATCCTTGGTGTTGCACGTCGGTGGATGCGCTTGTGG

CDAB_REF   CTTCCAGTTGGCCAAGGCAACTGAATACAAACCACAAAAAAAAAAAACAGAGCGAGTGGAA
Ax_w1118   CTTCCAGTTGGCCAAGGCAACTGAATACAAACCACAAAAAAAAAA-CAGAGCGAGTGGAA
A_w1118    CTTCCAGTTGGCCAAGGCAACTGAATACAAACCACAAAAAAAAAA-CAGAGCGAGTGGAA
AB_BAC     CTTCCAGTTGGCCAAGGCAACTGAATACAAACCACAAAAAAAAAAACAGAGCGAGTGGAA
DAB_BAC    CTTCCAGTTGGCCAAGGCAACTGAATACAAACCACAAAAAAAAA--CAGAGCGAGTGGAA
DA_BAC     CTTCCAGTTGGCCAAGGCAACTGAATACAAACCACAAAAAAAAA--CAGAGCGAGTGGAA
CDAB_BAC   CTTCCAGTTGGCCAAGGCAACTGAATACAAACCACAAAAAAAAA??CAGAGCGAGTGGAA
CDA_BAC    CTTCCAGTTGGCCAAGGCAACTGAATACAAACCACAAAAAAAAAAACAGAGCGAGTGGAA

CDAB_REF   TCGGAGGATGGCAATCGATGTAGGCAGCTTTTTCTGCCCTGAGTTTGTTATAATTTAGCC
Ax_w1118   TCGGAGGATGGCAATCGATGTAGGCAGCTTTTTCTGCCCTGAGTTTGTTATAATTTAGCC
A_w1118    TCGGAGGATGGCAATCGATGTAGGCAGCTTTTTCTGCCCTGAGTTTGTTATAATTTAGCC
AB_BAC     TCGGAGGATGGCAATCGATGTAGGCAGCTTTTTCTGCCCTGAGTTTGTTATAATTTAGCC
DAB_BAC    TCGGAGGATGGCAATCGATGTAGGCAGCTTTTTCTGCCCTGAGTTTGTTATAATTTAGCC
DA_BAC     TCGGAGGATGGCAATCGATGTAGGCAGCTTTTTCTGCCCTGAGTTTGTTATAATTTAGCC
CDAB_BAC   TCGGAGGATGGCAATCGATGTAGGCAGCTTTTTCTGCCCTGAGTTTGTTATAATTTAGCC
CDA_BAC    TCGGAGGATGGCAATCGATGTAGGCAGCTTTTTCTGCCCTGAGTTTGTTATAATTTAGCC

CDAB_REF   GACCAGCTCGTTTTTCTATTAATTAAAGCTGGCTGCAGACGTTGTCGCCGCCTGAAATAT
Ax_w1118   GACCAGCTCGTTTTTCTATTAATTAAAGCTGGCTGCAGACGTTGTCGCCGCCTGAAATAT
A_w1118    GACCAGCTCGTTTTTCTATTAATTAAAGCTGGCTGCAGACGTTGTCGCCGCCTGAAATAT
AB_BAC     GACCAGCTCGTTTTTCTATTAATTAAAGCTGGCTGCAGACGTTGTCGCCGCCTGAAATAT
DAB_BAC    GACCAGCTCGTTTTTCTATTAATTAAAGCTGGCTGCAGACGTTGTCGCCGCCTGAAATAT
DA_BAC     GACCAGCTCGTTTTTCTATTAATTAAAGCTGGCTGCAGACGTTGTCGCCGCCTGAAATAT
CDAB_BAC   GACCAGCTCGTTTTTCTATTAATTAAAGCTGGCTGCAGACGTTGTCGCCGCCTGAAATAT
CDA_BAC    GACCAGCTCGTTTTTCTATTAATTAAAGCTGGCTGCAGACGTTGTCGCCGCCTGAAATAT

CDAB_REF   TCTCACATAATTATTTACGATTTGACATAATCATCATCCTCGTCATCGGCGTCGTCCATT
Ax_w1118   TCTCACATAATTATTTACGATTTGACATAATCATCATCCTCGTCATCGGCGTCGTCCATT
A_w1118    TCTCACATAATTATTTACGATTTGACATAATCATCATCCTCGTCATCGGCGTCGTCCATT
AB_BAC     TCTCACATAATTATTTACGATTTGACATAATCATCATCCTCGTCATCGGCGTCGTCCATT
DAB_BAC    TCTCACATAATTATTTACGATTTGACATAATCATCATCCTCGTCATCGGCGTCGTCCATT
DA_BAC     TCTCACATAATTATTTACGATTTGACATAATCATCATCCTCGTCATCGGCGTCGTCCATT
CDAB_BAC   TCTCACATAATTATTTACGATTTGACATAATCATCATCCTCGTCATCGGCGTCGTCCATT
CDA_BAC    TCTCACATAATTATTTACGATTTGACATAATCATCATCCTCGTCATCGGCGTCGTCCATT
```

```
CDAB_REF   TAGAGCTGTGCTGCCATAACAGTTACAGTCTCCTCGATCGGGGGATTCATTAGTATGAGC
Ax_w1118   TAGAGCTGTGCTGCCATAACAGTTACAGTCTCCTCGATCGGGGGATTCATTAGTATGAGC
A_w1118    TAGAGCTGTGCTGCCATAACAGTTACAGTCTCCTCGATCGGGGGATTCATTAGTATGAGC
CDAB_BAC   TAGAGCTGTGCTGCCATAACAGTTACAGTCTCCTCGATCGGGGGATTCATTAGTATGAGC
DAB_BAC    TAGAGCTGTGCTGCCATAACAGTTACAGTCTCCTCGATCGGGGGATTCATTAGTATGAGC
DA_BAC     TAGAGCTGTGCTGCCATAACAGTTACAGTCTCCTCGATCGGGGGATTCATTAGTATGAGC
AB_BAC     TAGAGCTGTGCTGCCATAACAGTTACAGTCTCCTCGATCGGGGGATTCATTAGTATGAGC
CDA_BAC    TAGAGCTGTGCTGCCATAACAGTTACAGTCTCCTCGATCGGGGGATTCATTAGTATGAGC

CDAB_REF   AATAAATCGCTGGCTAGTCAGGATGGTTTCCTATGAACTTGAGTGTAGGTACGACTTTAT
Ax_w1118   AATAAATCGCTGGCTAGTCAGGATGGTTTCCTATGAACTTGAGTGTAGGTACGACTTTAT
A_w1118    AATAAATCGCTGGCTAGTCAGGATGGTTTCCTATGAACTTGAGTGTAGGTACGACTTTAT
CDAB_BAC   AATAAATCGCTGGCTAGTCAGGATGGTTTCCTATGAACTTGAGTGTAGGTACGACTTTAT
DAB_BAC    AATAAATCGCTGGCTAGTCAGGATGGTTTCCTATGAACTTGAGTGTAGGTACGACTTTAT
DA_BAC     AATAAATCGCTGGCTAGTCAGGATGGTTTCCTATGAACTTGAGTGTAGGTACGACTTTAT
AB_BAC     AATAAATCGCTGGCTAGTCAGGATGGTTTCCTATGAACTTGAGTGTAGGTACGACTTTAT
CDA_BAC    AATAAATCGCTGGCTAGTCAGGATGGTTTCCTATGAACTTGAGTGTAGGTACGACTTTAT

CDAB_REF   ATGTATGTACATATATATTTCACACGATGCCATCCCATATACCCATGAAAATTTACCTAT
Ax_w1118   ATGTATGTACATATATATTTCACACGATGCCATCCCATATACCCATGAAAATTTACCTAT
A_w1118    ATGTATGTACATATATATTTCACACGATGCCATCCCATATACCCATGAAAATTTACCTAT
CDAB_BAC   ATGTATGTACATATATATTTCACACGATGCCATCCCATATACCCATGAAAATTTACCTAT
DAB_BAC    ATGTATGTACATATATATTTCACACGATGCCATCCCATATACCCATGAAAATTTACCTAT
DA_BAC     ATGTATGTACATATATATTTCACACGATGCCATCCCATATACCCATGAAAATTTACCTAT
AB_BAC     ATGTATGTACATATATATTTCACACGATGCCATCCCATATACCCATGAAAATTTACCTAT
CDA_BAC    ATGTATGTACATATATATTTCACACGATGCCATCCCATATACCCATGAAAATTTACCTAT

CDAB_REF   TTTGAGCCAAAAATTGAAAGTGATAAAAGCAAACAAAAAAAAAGAGAGAATAGGTTAGA
Ax_w1118   TTTGAGCCAAAAATTGAAAGTGATAAAAGCAAACAAAAAAAA-GAGAGAATAGGTTAGA
A_w1118    TTTGAGCCAAAAATTGAAAGTGATAAAAGCAAACAAAAAAAA-GAGAGAATAGGTTAGA
CDAB_BAC   TTTGAGCCAAAAATTGAAAGTGATAAAAGCAAACAAAAAAAAAGAGAGAATAGGTTAGA
DAB_BAC    TTTGAGCCAAAAATTGAAAGTGATAAAAGCAAACAAAAAAAAAGAGAGAATAGGTTAGA
DA_BAC     TTTGAGCCAAAAATTGAAAGTGATAAAAGCAAACAAAAAAAAAGAGAGAATAGGTTAGA
AB_BAC     TTTGAGCCAAAAATTGAAAGTGATAAAAGCAAACAAAAAAAAAGAGAGAATAGGTTAGA
CDA_BAC    TTTGAGCCAAAAATTGAAAGTGATAAAAGCAAACAAAAAAAAAGAGAGAATAGGTTAGA

                           Ax-rev primer
CDAB_REF   TTTAAATGATGATCCTGGCAATCCTTGCTGGCATCTTGCGCATGCGTGACGCATTTCTAA
Ax_w1118   TTTAAATGATGATCCTGGCAATCCTTGCTGG-3'
A_w1118    TTTAAATGATGATCCTGGCAATCCTTGCTGGCATCTTGCGCATGCGTGACGCATTTCTAA
CDAB_BAC   TTTAAATGATGATCCTGGCAATCCTTGCTGGCATCTTGCGCATGCGTGACGCATTTCTAA
DAB_BAC    TTTAAATGATGATCCTGGCAATCCTTGCTGGCATCTTGCGCATGCGTGACGCATTTCTAA
DA_BAC     TTTAAATGATGATCCTGGCAATCCTTGCTGGCATCTTGCGCATGCGTGACGCATTTCTAA
AB_BAC     TTTAAATGATGATCCTGGCAATCCTTGCTGGCATCTTGCGCATGCGTGACGCATTTCTAA
CDA_BAC    TTTAAATGATGATCCTGGCAATCCTTGCTGGCATCTTGCGCATGCGTGACGCATTTCTAA

                                                    B-fwd primer
CDAB_REF   CGAGTTTGCCGACTCAAAGCGGATCGTATCGCATCCTTGGTCTTTCAGAAGGGGTTGAAC
 B_BAC                                             5'-TTTCAGAAGGGGTTGAAC
AB_BAC     CGAGTTTGCCGACTCAAAGCGGATCGTATCGCATCCTTGGTCTTTCAGAAGGGGTTGAAC
CDAB_BAC   CGAGTTTGCCGACTCAAAGCGGATCGTATCGCATCCTTGGTCTTTCAGAAGGGGTTGAAC
DAB_BAC    CGAGTTTGCCGACTCAAAGCGGATCGTATCGCATCCTTGGTCTTTCAGAAGGGGTTGAAC
A_w1118    CGAGTTTGCCGACTCAAAGCGGATCGTATCGCATCCTTGGTC-3'
CDA_BAC    CGAGTTTGCCGACTCAAAGCGGATCGTATCGCATCCTTGGTC-3'
DA_BAC     CGAGTTTGCCGACTCAAAGCGGATCGTATCGCATCCTTGGTC-3'
                                          A-rev primer
```

```
CDAB_REF   CACCATGCTTATGCAGATGAGTTGGTTCCCAGCTCTTGCCTCATCCTTTTTGTGTGCTTT
B_BAC      CACCATGCTTATGCAGATGAGTTGGTTCCCAGCTCTTGCCTCATCCTTTTTGTGTGCTTT
AB_BAC     CACCATGCTTATGCAGATGAGTTGGTTCCCAGCTCTTGCCTCATCCTTTTTGTGTGCTTT
CDAB_BAC   CACCATGCTTATGCAGATGAGTTGGTTCCCAGCTCTTGCCTCATCCTTTTTGTGTGCTTT
DAB_BAC    CACCATGCTTATGCAGATGAGTTGGTTCCCAGCTCTTGCCTCATCCTTTTTGTGTGCTTT

CDAB_REF   CGAGTTTTTTTTTTTTGCTCTGCTCAGCCTCTACGAAAAAAGGGTTAGGGTCCAGACGTC
B_BAC      CGAGTTTTTTTTTTT-GCTCTGCTCAGCCTCTACGAAAAAAGGGTTAGGGTCCAGACGTC
AB_BAC     CGAGTTTTTTTTTTT-GCTCTGCTCAGCCTCTACGAAAAAAGGGTTAGGGTCCAGACGTC
CDAB_BAC   CGAGTTTTTTTTTTT-GCTCTGCTCAGCCTCTACGAAAAAAGGGTTAGGGTCCAGACGCC
DAB_BAC    CGAGTTTTTTTTTTT-GCTCTGCTCAGCCTCTACGAAAAAAGGGTTAGGGTCCAGACGCC

CDAB_REF   CGTCGAGTTTTTTTTTTTTTTTGGGTAAGAAAAAGCGAATTTAATTAAAATTTTTTTCTT
B_BAC      CGTCGAGTTTTTTTTTTTTT--GGGTAAGAAAAAGCGAATTTAATTAAAATTTTTTTCTT
AB_BAC     CGTCGAGTTTTTTTTTTTTT--GGGTAAGAAAAAGCGAATTTAATTAAAATTTTTTTCTT
CDAB_BAC   CGTCGAGTTTTTTTTTTTTT--GGGTAAGAAAAAGCGAATTTAATTAAAATTTTTTTCTT
DAB_BAC    CGTCGAGTTTTTTTTTTTTT---GGGTAAGAAAAAGCGAATTTAATTAAAATTTTTTTCTT

CDAB_REF   ATAGGCGCGTAGCATTGTGAGAACGTCGCAGGCCAGAACTTAATAAATATCATTTTTTGC
B_BAC      ATAGGCGCGTgGCATTGTGAGAACGTCGCAGGCCAGAACTTAATAAATATCATTTTTTGC
AB_BAC     ATAGGCGCGTgGCATTGTGAGAACGTCGCAGGCCAGAACTTAATAAATATCATTTTTTGC
CDAB_BAC   ATAGGCGCGTAGCATTGTGAGAACGTCGCAGGCCAGAACTTAATAAATATCATTTTTTGC
DAB_BAC    ATAGGCGCGTAGCATTGTGAGAACGTCGCAGGCCAGAACTTAATAAATATCATTTTTTGC

                                B-rev primer
CDAB_REF   TGGAACTTCTTCAAGCCAGTTTCTTATGCATACG...
B_BAC      TGGAACTTCTTCAAGCCAGTTTCTTATGCATACG-3'
AB_BAC     TGGAACTTCTTCAAGCCAGTTTCTTATGCATACG-3'
CDAB_BAC   TGGAACTTCTTCAAGCCAGTTTCTTATGCATACG-3'
DAB_BAC    TGGAACTTCTTCAAGCCAGTTTCTTATGCATACG-3'
```